Am J Cancer Res 2025;15(7):2949-2969
www.ajcr.us /ISSN:2156-6976/ajcr0166700

Original Article

Increased autophagy activity suppresses hyperglycemia-related colorectal cancer tumorigenesis both *in vitro* and *in vivo*

Pei-Wen Lin[1], Yu-Wen Liu[1], Man-Ling Chu[1], Chien-An Chu[2], Chung-Ta Lee[2,3], Yao-Hsiang Shih[4], Sheng-Hui Lan[5], Shang-Ying Wu[6], Hong-Yi Chang[4], Wei-Chung Chen[7], I-Chen Wu[7,8], Li-Tzong Chen[7,8], Ming-Yii Huang[8,9,10], Jaw-Yuan Wang[8,11,12,13,14], Ying-Ray Lee[1,15,16,17,18], Hsiao-Sheng Liu[1,8,19]

[1]Master of Science Program in Tropical Medicine, College of Medicine, Kaohsiung Medical University, Kaohsiung, Taiwan; [2]Department of Pathology, National Cheng Kung University Hospital, Tainan, Taiwan; [3]Department of Pathology, National Cheng Kung University Hospital Dou-Liou Branch, Douliou City, Yunlin County, Taiwan; [4]Department of Anatomy, School of Medicine, College of Medicine, Kaohsiung Medical University, Kaohsiung, Taiwan; [5]Department of Life Sciences and Institute of Genome Sciences, National Yang Ming Chiao Tung University, Taipei, Taiwan; [6]Department of Microbiology and Immunology, School of Medicine, College of Medicine, Taipei Medical University, Taipei, Taiwan; [7]Division of Gastroenterology, Department of Internal Medicine, Kaohsiung Medical University Hospital, Kaohsiung, Taiwan; [8]Center for Cancer Research, Kaohsiung Medical University, Kaohsiung, Taiwan; [9]Department of Radiation Oncology, Kaohsiung Medical University Hospital, Kaohsiung Medical University, Kaohsiung, Taiwan; [10]Department of Radiation Oncology, School of Medicine, College of Medicine, Kaohsiung Medical University, Kaohsiung, Taiwan; [11]Division of Colorectal Surgery, Department of Surgery, Kaohsiung Medical University Hospital, Kaohsiung Medical University, Kaohsiung, Taiwan; [12]Department of Surgery, Faculty of Medicine, College of Medicine, Kaohsiung Medical University, Kaohsiung, Taiwan; [13]Graduate Institute of Clinical Medicine, College of Medicine, Kaohsiung Medical University, Kaohsiung, Taiwan; [14]Graduate Institute of Medicine, College of Medicine, Kaohsiung Medical University, Kaohsiung, Taiwan; [15]Department of Microbiology and Immunology, College of Medicine, Kaohsiung Medical University, Kaohsiung, Taiwan; [16]Faculty of Post-Baccalaureate Medicine, College of Medicine, Kaohsiung Medical University, Kaohsiung, Taiwan; [17]Center for Tropical Medicine and Infectious Disease, Kaohsiung Medical University, Kaohsiung, Taiwan; [18]Department of Medical Research, Kaohsiung Medical University Hospital, Kaohsiung, Taiwan; [19]Medical Research Center, Kaohsiung Medical University Hospital, Kaohsiung Medical University, Kaohsiung, Taiwan

Received June 11, 2025; Accepted July 14, 2025; Epub July 15, 2025; Published July 30, 2025

Abstract: Hyperglycemia contributes to recurrence, poor survival, and drug resistance in colorectal cancer (CRC) patients. Overexpression of G9a (euchromatic histone-lysine N-methyltransferase 2, EHMT2), together with decreased autophagy activity, has been implicated in promoting CRC tumorigenesis and chemoresistance. Here, we demonstrate that high glucose (25 mM) enhances proliferation, focus formation, and migration of CRC cells, while concurrently suppressing autophagy activity. Importantly, pharmacological induction of autophagy increases CRC cell sensitivity to chemotherapeutic agents (5-fluorouracil and oxaliplatin) and attenuates high glucose-induced tumorigenic behaviors. Analysis of CRC patient specimens and data from the TCGA COAD database revealed that LC3, an autophagy marker, is elevated in tumor tissues compared to adjacent normal tissues, and that high LC3 mRNA expression correlates with poor overall survival. Furthermore, enhancing autophagy via the autophagy inducer rapamycin significantly suppressed high glucose-induced tumor formation in a CRC xenograft mouse model. In addition, we identified niclosamide (NC), a repurposed antihelminthic agent, and its derivative niclosamide ethanolamine (NEN), as potential G9a inhibitors and autophagy inducers. NEN dose-dependently suppressed high glucose-activated oncogenic signaling pathways, including β-catenin, c-Myc, STAT3, G9a, and cyclin D1, while restoring autophagy activity. Collectively, our *in vitro* and *in vivo* findings strongly support that enhancing autophagy represents a multifaceted strategy to alleviate hyperglycemia, inhibit G9a-mediated signaling, increase chemosensitivity, and suppress high glucose-driven CRC tumorigenesis.

Keywords: Autophagy, colorectal cancer, hyperglycemia, niclosamide ethanolamine

https://doi.org/10.62347/XSRQ4118

Introduction

Colorectal cancer (CRC) ranks among the most common malignancies and is associated with poor five-year survival rates, with nearly half of patients developing distant metastases despite standard treatment protocols [1]. Epidemiological studies have revealed a strong association between CRC progression and hyperglycemia, a common complication of diabetes mellitus [2-6]. Hyperglycemia promotes CRC cell proliferation, metastasis, and drug resistance, particularly to oxaliplatin [5]. Meanwhile, autophagy, a cellular degradation and recycling mechanism, plays a complex role in cancer progression and treatment resistance [7, 8]. Notably, increasing autophagy activity has been linked to both tumor suppression and improved therapeutic responses in CRC and diabetic conditions [9-16]. Understanding the interplay between autophagy, hyperglycemia, and CRC tumorigenesis is critical for developing more effective therapies.

Autophagy is a lysosomal degradation process that maintains cellular homeostasis by recycling damaged organelles, proteins, and microRNAs. Functionally, it is categorized into conventional degradative autophagy and unconventional secretory autophagy. The former protects cells under stress by degrading intracellular contents, while the latter exports selected cargoes through autophagosome-like vesicles, bypassing the endoplasmic reticulum-Golgi route [17-20]. This unconventional pathway is implicated in various diseases, including cancers and metabolic syndromes [18]. Autophagy serves as a double-edged sword in tumorigenesis, playing distinct roles depending on the stage and cellular context of cancer. In the early stages, knockout of autophagy-related genes (ATGs) in mice leads to tumorigenic phenotypes [7], and that Beclin1, a core autophagy gene, is often downregulated in colorectal cancer (CRC), where its restoration suppresses tumor growth [15]. Furthermore, specific autophagy inhibitors or repressors, such as miR-338-5p, can promote tumor development and metastasis through suppression of autophagy via targets like PIK3C3 [11]. We have shown that autophagy can inhibit Ha-*ras*-driven tumorigenesis by limiting proliferation [21], and that pharmacological activation of autophagy through agents such as rapamycin and amiodarone can suppress CRC progression both *in vitro* and *in vivo* [11, 22]. Jeong *et al.* (2019) also demonstrated that combining oxaliplatin with docosahexaenoic acid enhances autophagic cell death in CRC, further highlighting autophagy's therapeutic potential [23].

Autophagy frequently promotes tumor development, growth, and survival in established or advanced malignancies [24]. This pro-tumor function involves several mechanisms including to support the high metabolic demands of cancer cells by supplying necessary nutrients under challenging conditions like hypoxia [25]. Autophagy also prevents cancer cell death during treatment, inducing dormancy, promoting recurrence and metastasis, and impeding therapeutic efficacy by contributing to drug resistance [25]. Furthermore, autophagy can promote metastasis by enhancing resistance to apoptosis and is strongly correlated with the survival and maintenance of cancer stem cells [25]. In the context of immunity, autophagy may support immune evasion by acting as a tumor protector, potentially through mechanisms like the degradation of MHC-I, which is observed in pancreatic cancer [26], or by protecting tumor cells from T cell-mediated cytotoxicity [25]. This pro-survival role in RAS-mutated cancers (including lung, colon, and pancreatic) and its link to advanced stages of various cancers underscore its significance in therapeutic resistance and progression. Therefore, understanding how autophagy facilitates these aspects in specific cancer contexts is crucial for developing effective treatments that target this pathway [25].

Hyperglycemia is increasingly recognized as a critical factor in cancer progression. Cohort studies have linked high blood glucose levels to increased risks for pancreatic and colorectal cancers [3]. Hyperglycemia is an etiological factor for poor outcomes and shorter overall survival in glioblastoma multiforme (GBM) patients [4]. In CRC, hyperglycemia is associated with oxaliplatin resistance and reduced survival [5, 6]. Mechanistic studies show that hyperglycemia enhances CRC malignancy via the ERK-αvβ6 signaling pathway [2] and by remodeling the hexosamine biosynthetic pathway (HBP), thereby facilitating immune evasion [27, 28]. Hyperglycemia also undermines the efficacy and safety of immune checkpoint therapies in breast cancer [29]. In pancreatic cancer, high glucose enhances sphere formation and tumor-

igenicity [30], while in prostate cancer, it promotes matrix metalloproteinase (MMP) expression [31]. These findings reflect the diverse and cancer-specific effects of hyperglycemia.

G9a, a histone methyltransferase, is overexpressed in several malignancies, including CRC, gastric, ovarian, and esophageal cancers [32]. It epigenetically regulates gene expression to promote proliferation, survival, and invasion. G9a knockdown suppresses tumor growth and induces chromosomal instability, underscoring its therapeutic potential [32]. Moreover, G9a expression has been associated with hyperglycemia in type 1 diabetes [33], suggesting a possible mechanistic link between epigenetic regulation and metabolic disorders.

In the context of CRC, increasing autophagy activity not only suppresses tumor progression but also restores glucose homeostasis and overcomes chemoresistance [10, 16]. Cheng *et al.* (2025) demonstrated that statins (pitavastatin and atorvastatin) suppress the growth of high-glucose-adapted CRC cells by inducing autophagy and enhancing 5-FU cytotoxicity via the PERK/ATF4/CHOP signaling axis [9]. These findings highlight autophagy's central role in hyperglycemia-related tumorigenesis and therapy resistance.

Type 2 diabetes mellitus (T2DM), characterized by insulin resistance and hyperglycemia, is commonly managed by increasing insulin secretion or sensitivity [34]. Autophagy is essential for pancreatic β-cell homeostasis and insulin secretion. Deficiency of autophagy genes like *Atg7* leads to hyperglycemia, reduced β-cell mass, and impaired insulin output [12-14, 35-37]. Niclosamide, a repurposed anthelmintic drug, was found to induce autophagy and promote insulin secretion, improving glycemic control *in vitro* and *in vivo* [38]. These observations support the hypothesis that autophagy contributes to blood glucose regulation through pancreatic β-cell modulation.

As a nutrient sensor, autophagy is activated under conditions of starvation or energy deprivation. The process degrades cytosolic contents to supply amino acids and fatty acids for energy production [39, 40]. Interestingly, while starvation induces autophagy in most cells, β-cells suppress autophagy under such conditions but activate it in response to high glucose [41, 42]. This suggests a cell-type-specific regulation of autophagy based on nutrient status.

Altogether, these studies indicate that autophagy plays a multifaceted role in regulating glucose metabolism, insulin secretion, tumor progression, and treatment responses. However, the precise mechanisms by which autophagy influences hyperglycemia-related CRC development and chemoresistance remain unclear and merit further investigation.

Although autophagy has been extensively studied in the context of cancer and diabetes, the precise mechanisms by which autophagy regulates hyperglycemia-related CRC tumorigenesis and chemoresistance remain largely unexplored [5, 9-11, 16]. While autophagy appears to influence insulin secretion and glucose metabolism via pancreatic β-cells [12-14, 35-38], it is still unclear how these systemic metabolic effects impact CRC progression in hyperglycemic patients. Furthermore, the involvement of epigenetic factors such as G9a in linking hyperglycemia, autophagy, and CRC metastasis has not been elucidated [32, 33]. Thus, a mechanistic investigation into the autophagy-mediated signaling pathways that bridge hyperglycemia and CRC malignancy is urgently needed.

This study proposes a comprehensive approach to investigate the role of autophagy in hyperglycemia-associated CRC tumorigenesis and chemoresistance. We begin by establishing *in vitro* CRC models under high-glucose culture conditions to mimic the diabetic microenvironment. Autophagy activity, blood insulin level, and key metabolic regulators will be assessed using Western blotting, CRISP/Cas9, ELISA, and immunofluorescence microscopy. Next, we will assess whether autophagy inducers such as rapamycin and niclosamide can restore autophagic flux and suppress CRC cell proliferation and migration in high-glucose environments. These interventions will be evaluated alone and in combination with 5-FU or oxaliplatin to determine their effects on drug sensitivity. Autophagy dependency will be confirmed via genetic manipulation (e.g., *Atg5* knockout or siRNA knockdown). We will use the animal model of hyperglycemia with CRC to validate the role of autophagy observed *in vitro*. Finally, clinical relevance will be addressed by analyzing CRC patient tissue samples, correlating LC3

expression level with CRC patient tumor and multiply clinical parameters. These investigations will clarify how autophagy modulates CRC progression under hyperglycemia conditions.

Materials and methods

Cell lines and reagents

Human CRC cell lines SW480 and HCT-116 were purchased from Bioresource Collection and Research Center (Hsinchu, Taiwan) and cultured with low-glucose Dulbecco's modified Eagle medium (DMEM, 5 mM Glucose, Gibco, 11885-084) supplemented with 10% fetal bovine serum (FBS, Gibco, 10437-028) and Pen Step (100 Units/mL penicillin + 100 μg/mL Streptomycin, Gibco, 15140-122). Cells were incubated at 37°C in a 5% CO_2 incubator. High-glucose DMEM was purchased from Gibco (25 mM Glucose, 11965-092). Niclosamide ethanolamine salt (NEN, LGC Standards, TRC-N395505), rapamycin (Sigma-Aldrich, R0395), Tat-Beclin 1 D11 (Tat-D11, Novus Biologicals, NBP2-49888), 10058-F4 (Selleck Chemicals, S7153), PNU-74654 (Selleck Chemicals, S8429), and Cryptotanshinone (Tanshinone C, Selleck Chemicals, S2285) were purchased.

Immunoblotting analysis

After various treatments, the cells (1×10^6) were lysed with 100 μl of Lysate-RIPA buffer, and the total protein from the cell lysate was collected. For Western blotting, the lysates (30 μg protein) were electrophoretically separated by sodium dodecyl sulfate-polyacrylamide gel electrophoresis (SDS-PAGE) and transferred to a polyvinylidene fluoride (PVDF) membrane (Millipore, ISEQ85R). The membrane was blocked with 5% skimmed milk in PBST [sodium chloride (100 mM), disodium hydrogen phosphate (80 mM), sodium dihydrogen phosphate (20 mM), Tween 20 (0.2%), pH 7.5] for 1 h. The membrane was incubated with the primary antibody (LC3, 1:1000, MLB, PM036; β-catenin, 1:1000, Cell Signaling, 9562; Phospho-β-catenin (Ser675), 1:1000, Cell Signaling, 4176; c-Myc, 1:1000, Cell Signaling, 5605; EHMT2-G9A, 1:1000, abcam, ab185050; Cyclin D1, 1:1000, abcam, ab134175; ATG5, 1:1000, abcam, ab108327; Phospho-SRAT3 (Tyr705), 1:1000, Cell Signaling, 9145; STAT3, 1:1000, Cell Signaling, 9139; CD133, 1:1000, GeneTex, GTX100567; CD44, 1:1000, GeneTex, GTX102111; Nanog, 1:1000, Cell signaling, 4893S; OCT4, 1:1000, Cell signaling, 2750S; p62 (SQSTM1), 1:1000, MLB, PM045; GAPDH, 1:10000, GeneTex, GTX100118) at 4°C overnight. After washing with PBST, the membrane was hybridized with an HRP-conjugated secondary antibody (Thermo Fisher Scientific, 31460 and 31430) at RT for 1 h. The membrane was exposed to an imaging system to detect signals using chemiluminescence. Views were quantified by ImageJ software.

Immunofluorescent staining

Cells (1×10^5/well) were seeded on a slide. Cells under different conditions were then fixed in 4% formaldehyde for 20 min. The slide was incubated for 30 min in 0.1% Triton X-100 in PBS. Anti-LC3 antibodies (1:50, MBL, M152-3) will be added to the slide and left overnight at 4°C. The primary antibody was visualized using an appropriate secondary antibody (Thermo Fisher Scientific, A11001). The fluorescent change of the cells was investigated under a confocal microscope (FV-1000; Olympus).

Immunohistochemical staining (IHC)

The paraffin sections slides were treated with anti-LC3 (1:300, MBL, PM036) and anti-Ki67 (1:250, Sigma-Aldrich, AB9260) antibodies followed by labeling with the secondary antibody for 30 min at RT [19]. The slides were treated with diaminobenzidine (DAB) solution for 10 min at RT and counterstained with 10% hematoxylin (Muto Pure Chemicals Co., LTD, 3000-2).

Small hairpin RNA (shRNA) lentiviral infection system

Cells were infected with lentivirus containing sh*GFP* RNA (Academia Sinica, TRCN000007-2181), sh*Atg5* RNA (Academia Sinica, TRCN-0000151474), or sh*EHMT2* RNA (Academia Sinica, TRCN0000115669) and incubated overnight. Stable cell lines were selected by puromycin treatment for 2 weeks.

CRISPR-Cas9 system

This system consists of two steps: (a) CRISPR/Cas9 RNP electroporation: SW480 cells were synchronized with 200 ng/ml nocodazole for 17 h, followed by Cas9/gRNA (for specific gene target) delivery through electroporation. On the

day of electroporation, an equal volume of cRNA and tracrRNA was mixed to prepare the gRNA complex solution (150 pmol). Cas9 protein (30 pmol) and Cas9/gRNA (150 pmol) were mixed in Opti-MEM ™ I Reduced Serum Medium (ThermoFisher, #31985062) at RT for 15 min to form Cas9/gRNA ribonucleoprotein (RNP). At the same time, 1×10^5 of synchronized cells were collected by centrifugation, washed with Opti-MEM twice, and then re-suspended in the optimal volume of Opti-MEM, followed by adding Cas9/gRNA RNP. The RNP was delivered into the cell through the NEPA21 Electroporator™. (b) Evaluation of gene editing efficiency by T7E1 digestion and high-resolution melting (HRM) analysis: The electroporated cells were transferred immediately to 24-well culture dishes containing 1 ml of the corresponding culture medium and then incubated in a 37°C, 5% CO_2 incubator. After 48 h recovery, we performed T7E1 and high-resolution melting to validate gene editing efficiency. Moreover, a limited dilution was carried out by seeding cells at 0.5 cells/well density. After two weeks of incubation, some single-cell clones were used for HRM-qPCR analysis to check for mutations in both target genes.

MTT assay

Cells (1×10^5/well) in 96-well plates received different treatments for 1 to 5 days. MTT solution (Sigma, M2128) (0.5 mg/ml in DMEM medium) was added to each well at 37°C for 3 h. The medium was removed, and 100 µl of DMSO (Sigma, D4540) was added. Cell proliferation was determined by measuring the cell lysate at the optical density of 570 nm wavelength using a 96-well Thermo Scientific™ Multiskan Sky Microplate Spectrophotometer.

Focus formation assay

Cells received different glucose concentration medium treatments for 5 days. The 1000 cells plated into the 6 cm culture dish received other treatments and were cultured for 7 days to allow colony formation. Then cells were fixed with 4% formaldehyde and stained with 0.4% crystal violet (Sigma, V5265). Cells were then lysed with 2% SDS solution and measured at an optical density at 570 nm wavelength.

Wound healing assay

Cells were seeded in a 2-well culture insert, which was placed on a 12-well plate. Cells were treated with 1 µM NEN or 150 nM rapamycin in different glucose concentration mediums, and inserts were removed on day 4. Wash each well with 1X PBS on day 5 to remove residual cell debris. The wound healing was observed under microscopy. Views were quantified by ImageJ software.

Sphere formation assay

SW480 cells were pretreated 1 µM NEN for 24 h in DMEM containing 5 or 25 mM glucose, detached with 0.25% Trypsin/2.21 mM EDTA (Corning), and plated at 3,000 cells/well in 6-well ultra-low adhesion plates (Corning) with sphere formation medium (SFM). SFM, a crucial component for promoting sphere formation, consisted of serum-free 5 or 25 mM glucose DMEM supplemented with 1x B27 supplement (Gibco, 17504044), 20 ng/mL epidermal growth factor (EGF) (Sigma, E4127), and 20 ng/mL basic fibroblast growth factor (bFGF) (Gibco, 100-18B-50UG). Media were re-supplemented every 3 days until 7 days of growth, and the spheres were collected for immunoblotting.

Tissue microarray (TMA) of CRC specimens

CRC patient specimens used in the study were approved by the Institutional Review Board of the Kaohsiung Medical University Hospital (KMUH) (IRB document number: KMUHIRB-G(I)-20210047) and the Institutional Review Board of National Cheng Kung University Hospital (Approval No. A-ER-108-535). The research methods conformed to the standards set by the Declaration of Helsinki. CRC specimens were obtained from KMUH and National Cheng Kung University Hospital. A total of 14 CRC tissue array slides were used, including 61 normal tissues and 209 tumor specimens. The analysis of human tissue sections in adjacent normal and tumor parts was performed using paraffin-embedded CRC specimens in the tissue array.

Tissue microarray (TMA) score

Positive IHC staining of the tissue sections was obtained by multiplying the intensity and percentage scores, ranging from 0 to 9. The staining percentage was scored as follows: 0, 0% immunoreactive cells; 1, detectable dots in <5% of cells; 2, readily detectable dots in 5-50% of cells; 3, dots in >50% of cells. The intensity score was defined as 0 (no staining), 1

(weak staining), 2 (moderate staining), and 3 (strong staining) [43, 44]. All IHC slides were scored by a professionally trained and certified pathologist who was blinded to clinical data. Since a single rater performed the assessments, inter-rater reliability was not applicable.

CRC mice models

Male nude mice (4 weeks old) were obtained from the National Laboratory Animal Center, Taipei, Taiwan. The mice were maintained in a pathogen-free facility under isothermal conditions with regular photoperiods in the KMU Center for Laboratory Animals. Institutional Animal Care and Use Committee (IACUC) Animal experimental procedures were approved by the Institute of Animal Care and Use Committee at Kaohsiung Medical University (Affidavit of Approval of Animal Use Protocol No. 109134) and performed following the Guide for the Care and Use of Laboratory Animals [Guide for the Care and Use of Laboratory Animals (8th Edition)]. Mice (n=18, aged 7 weeks) were randomly divided into a control diet group (CD; containing 10% animal fat) (TestDiet, St Louis, Mo, catalog #58Y2) and a high-fat diet group (HFD, containing 60% animal fat) (TestDiet, catalog #58Y1). We used these diets in murine studies of obesity [45]. Body weight and blood glucose were measured weekly throughout the study.

Xenograft mouse model: Male nude mice fed control and high-fat diets for 11 weeks were inoculated with cells (2×10^6 cells in 100 µl of PBS) subcutaneously on the back of the mice. The tumor volume was measured according to the following formula: Tumor volume (mm^3) = length (mm) × $width^2$ (mm^2) ×0.5. The mice were divided into the following groups: (i) SW480 cell (CD), (ii) SW480 cell (HFD), and (iii) SW480 cell (HFD) plus autophagy inducer. Each group contained 6 mice.

Insulin detection

Blood was collected by a cardiac bleed into tubes containing heparin as an anticoagulant, and the plasma fraction was separated. The plasma was collected to measure insulin concentration with the Mercodia Mouse Insulin ELISA kit (Mercodia AB, 10-1247-01).

Quantification and statistical analysis

The results of the western blot assay were quantified using ImageJ software. Data were computed using the GraphPad Prism ver. 10.3.1 (GraphPad Software, Inc., San Diego, CA, USA). All data are presented as the mean ± SD. Differences between the experimental and control groups were analyzed by a two-tailed Student's *t*-test, one-, or two-way ANOVA with Turkey's multiple comparison test. The symbol represents *: $P<0.05$; **: $P<0.01$ and ***: $P<0.001$.

Results

The effect of high glucose on the autophagy activity and cell viability of CRC cells

Initially, we clarified the effect of high glucose on the autophagy activity of CRC cells. We investigated the level of the autophagy representative protein LC3 in CRC SW480 and HCT116 cell lines incubated with 5 (normal, 90 mg/dl blood sugar), 15 (diabetes, 270 mg/dl blood sugar), or 25 mM (over+, 450 mg/dl blood sugar) glucose-containing media for short (1 day) and long (5 days) times. Our results consistently demonstrated a dose-dependent decrease of LC3-II levels (representing autophagic vesicles) in SW480 and HCT116 cells by Western blotting (**Figure 1A**) and image analysis for GFP puncta formation of LC3 protein under a fluorescent microscope (**Figure 1B**). These results indicate that increasing glucose concentration may decrease autophagy activity in CRC cells from 1 to 5 days.

It is known that high glucose increases CRC cell viability and chemoresistance [5]. Similarly, we confirmed that both SW480 and HCT116 cell lines showed significant increase of cellular viability under high glucose (25 mM) conditions compared to low glucose (5 mM) at 72 h by MTT assay (**Figure 1C** and **1D**).

The effect of inducing autophagy activity on CRC cell viability and the sensitivity of CRC cells to anti-cancer drug treatment under high glucose conditions

We are interested in clarifying whether inducing autophagy activity by various inducers can affect CRC cell viability under high glucose conditions. Three autophagy inducers, niclosamide ethanolamine salt (NEN), rapamycin, and Tat-D11, were used to induce the autophagy activity of SW480 and HCT116 cells. Balgi *et al.* (2009) reported that niclosamide is a potential autophagy inducer and mTOR inhibitor [46]. NEN, a salt form of niclosamide, has higher util-

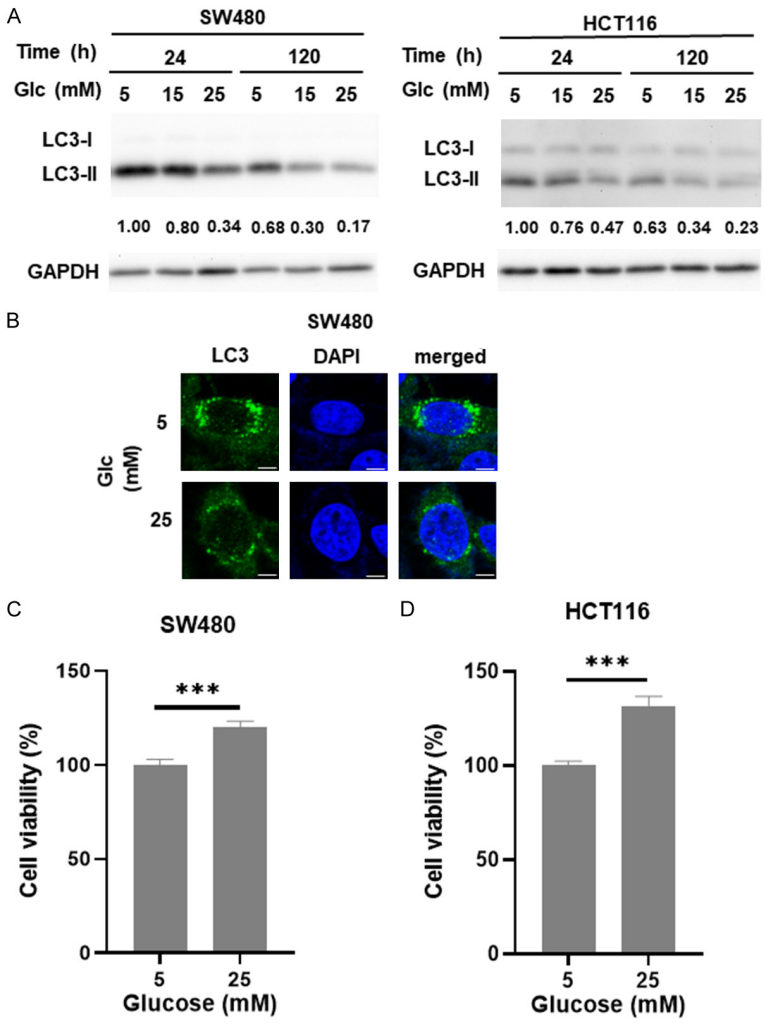

Figure 1. The effect of high glucose on the autophagy activity and cell viability of CRC cell lines. (A) SW480 and HCT116 cells were incubated in 5, 15, or 25 mM glucose (Glc) containing media for 1 day and 5 days. Cell lysates were investigated for LC3 protein level by Western blotting using the anti-LC3 antibody. GAPDH was used as the internal control. (B) LC3 protein was labeled by FITC-conjugated anti-LC3 antibody, and the nucleus was labeled by DAPI in SW480 cells maintained in 5 or 25 mM glucose medium for 1 day and investigated under a confocal fluorescent microscope. Scale bar =5 um. (C) SW480 cells and (D) HCT116 cells were incubated in 5 or 25 mM glucose-containing media for 72 h. Cell viability was determined by MTT assay at 570 nm wavelength. Error bars represent mean ± SD. Data were analyzed by Student's t-test. ***: P<0.001.

ity than niclosamide because it is high solubility in water, low toxicity, and orally bioavailable *in vivo*. Tat-D11 (Tat-Beclin 1 D11, Novus) is a highly specific autophagy inducing peptide. Rapamycin is an antifungal antibiotic and mTOR inhibitor. We confirmed that the LC3-II level was induced in a dose-dependent manner by three autophagy inducers under high glucose conditions (**Figure 2A-F**, upper panel). We then used the optimal dose of NEN (1 μM), rapamycin (150 nM), and Tat-D11 (5 μM) to enhance the autophagy activity of these CRC cell lines under high glucose conditions to clarify whether increased autophagy activity affects CRC cell viability determined by MTT assay. We reveal that the viability of both CRC cell lines was suppressed at 48 h post-treatment under high glucose conditions (**Figure 2A-F**, lower panel). To further confirm the suppressive effect of autophagy on CRC cell viability, we blocked autophagy activity by either genetic silencing (Figure S1A and S1C) or CRISPR-Cas9 knockout of *Atg5* gene under high glucose conditions (Figure S1B). We established various stable *Atg5* knockout clones. SW480-C19 is the heterologous *Atg5* knockout clone, SW480-C10, C12, C20 are homologous *Atg5* knockout clones (Figure S1B). We found that HCT116 cell viability was increased by silencing the *Atg5* gene at 72 h under high glucose conditions (Figure S1F), but this phenomenon was not significant for SW480 cells (Figure S1D). Likewise, the viability of SW480 *Atg5* knockout clones was also increased at 72 h under high glucose conditions (Figure S1E). In summary, the suppressive effect of autophagy on cancer cell viability was reversed while the autophagy gene was silenced or knocked out under high glucose conditions. It indicates that autophagy plays a suppressive role in CRC cell viability under high glucose conditions.

We found that SW480 and HCT116 cells after 5-fluorouracil (5-FU, 1 μg/ml) or oxaliplatin (Oxa, 7.5 μg/ml) treatment for 24 h, endogenous LC3-II was increased to various levels (Figure S2A-D, upper panel) under high glucose

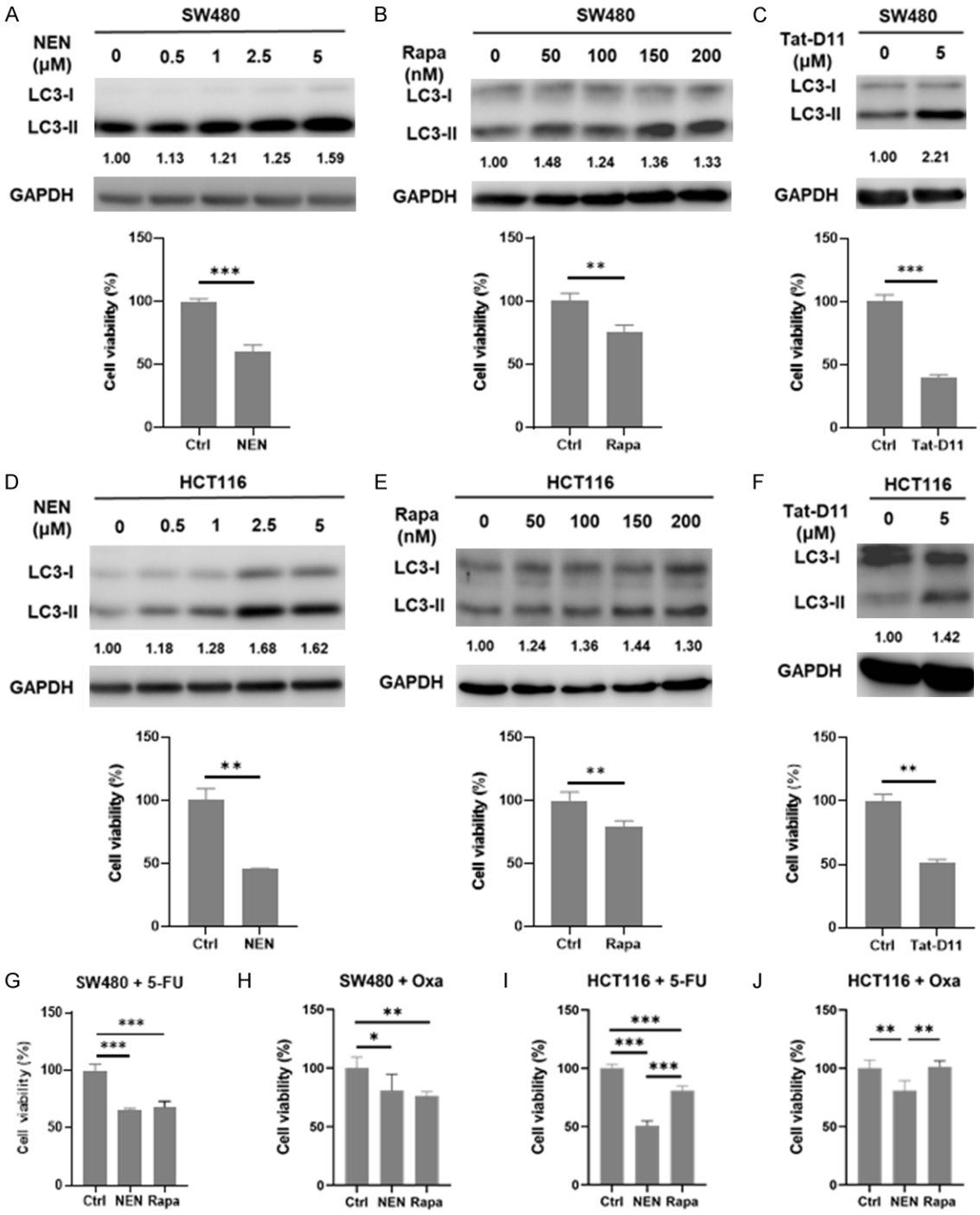

Figure 2. The effect of enhancing autophagy activity on CRC cell viability and sensitivity to anti-cancer drugs under high glucose conditions. (A-C) SW480 cells and (D-F) HCT116 cells were maintained in high glucose media with different concentrations of autophagy inducers for 24 h. LC3 protein levels were determined by Western blotting using the specific anti-LC3 antibody. GAPDH was used as the internal control. Cells were further treated with 1 μM niclosamide ethanolamine salt (NEN; A, D), 150 nM rapamycin (Rapa; B, E), or 5 μM Tat-D11 (C) and (F) for 48 h followed by MTT assay to determine the cell viability. (G, H) SW480 cells and (I, J) HCT116 cells were treated with 150 nM rapamycin (Rapa) or 1 μM NEN combined with 1 μg/ml 5-fluorouracil (5-FU; G and I) or 7.5 μg/ml oxaliplatin (Oxa; H and J) for 48 h. Cell viability was determined by MTT assay. Error bars represent mean ± SD. Data were analyzed by Student's t-test or one-way ANOVA. *: $P<0.05$; **: $P<0.01$; ***: $P<0.001$.

conditions, indicating that anti-cancer drugs enhance autophagy activity of CRC cells under high glucose conditions. Moreover, cell viability was significantly decreased after 5-FU or Oxa treatment compared to the control group under high glucose conditions (Figure S2A-D, lower panel).

We then investigated whether enhancing autophagy activity affects CRC cell sensitivity to anti-cancer drugs under high glucose conditions. Initially, we elevated the autophagy activity using NEN (1 μM) or rapamycin (Rapa, 150 nM) followed by measuring the cellular viability using MTT assay. Our data showed that NEN-induced autophagy increased the sensitivity of SW480 and HCT116 cells to 5-FU (1 μg/ml) and Oxa (7.5 μg/ml) under high glucose conditions (**Figure 2G-J**). However, rapamycin-induced autophagy could not increase the sensitivity of HCT116 cells to Oxa (**Figure 2J**).

Consistent with the above result, silencing *Atg5* gene expression by lentiviral shRNA significantly decreased the sensitivity of SW480 and HCT116 cells to 5-FU as well as Oxa compared to shGFP control cells (Figure S3A, S3B, S3D, and S3E). In contrast, knockout of *Atg5* gene by CRISP/Cas9 system further sensitizes SW480-C20 cells to 5-FU and Oxa treatment (Figure S3C and S3F). Altogether, the above findings suggest that boosting autophagy activity further sensitizes CRC cells to anti-cancer drugs in a high-glucose environment. Intriguingly, abolishing endogenous autophagy also enhances CRC cell sensitivity to anti-cancer treatment.

The effect of glucose concentration and autophagy activity on focus formation, migration, and sphere formation of CRC cells

Tumor cells with increased tumorigenicity may form foci in a plate. Focus formation (anchorage-dependent colony formation) was used to evaluate the effect of autophagy on CRC cell tumorigenesis under high glucose conditions. Initially, we found that high glucose (25 mM, HG) medium increased the number of focus formations compared to low glucose medium (5 mM, LG). The SW480 cells were then incubated with 5 or 25 mM glucose medium with autophagy either induced by rapamycin, NEN or abolished by knockout of the *Atg5* gene (SW480-C20). We found that increased autophagy by rapamycin or NEN significantly suppressed focus formation in either 5 or 25 mM glucose medium (**Figure 3A**). However, focus formation suppressed by enhancing autophagy activity was not blocked by knockout of the *Atg5* gene in SW480-C20 cells under 5- or 25-mM glucose medium (Figure S4A). These data suggest that the suppression of colony formation through enhanced autophagy activity depends on endogenous autophagy function.

Furthermore, we assessed how glucose concentration and enhanced autophagy affect CRC cell migration by wounding healing assay. We showed that SW480 and HCT116 cells cultured in high glucose (25 mM) medium showed higher cell migration than in low glucose (5 mM) medium (**Figures 3B** and S4B). Despite high glucose suppresses autophagy and enhances the motility of CRC cells, the effect of enhanced autophagy on cell motility remains unclear. Therefore, we treated CRC cells with the autophagy inducer (NEN or Rapa) for 24 h and found that high glucose increased CRC cell motility was significantly suppressed by increased autophagy activity using two inducers (**Figures 3B** and S4B).

Moreover, sphere formation is a characteristic of cancer cell stemness. It has been reported that high glucose promotes sphere and tumor formation of pancreatic cancer [30]. We clarified whether glucose concentration and enhanced autophagy activity affect cancer cell stemness. In contrast to Sato *et al.* (2020) report [30], we found that high glucose suppressed CRC cell sphere formation compared to low glucose (**Figure 3C**). Increased autophagy, induced by rapamycin (Rapa) or NEN, suppressed sphere formation in both low- and high-glucose media (**Figure 3C**). These data suggest that autophagy inducers can reduce stem-related sphere formation and high-glucose-induced focus formation and migration in CRC cells.

Signaling pathways involved in high glucose and NEN treatment of CRC cells

G9a histone methyltransferase affects tumorigenesis of many cancer cells, and is overexpressed in various cancers including CRC, therefore, small molecule inhibitors have been developed including BIX01294 [32]. Using BIX01294 we predicted a novel G9a inhibitor

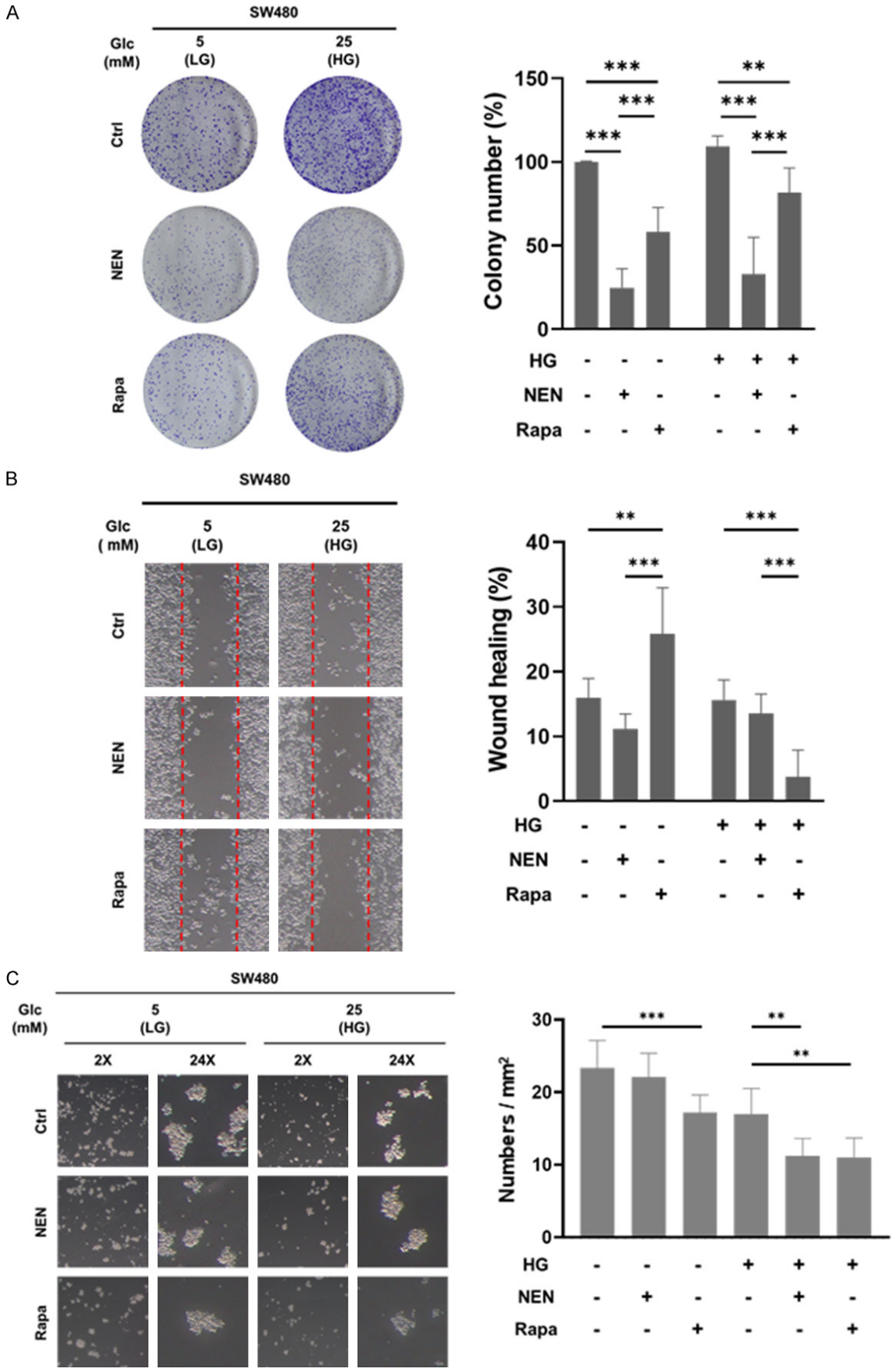
A
SW480
Glc (mM)
5 (LG)
25 (HG)
Ctrl
NEN
Rapa
Colony number (%)
150
100
50
0
***
***
***
**
***
***
HG - - - + + +
NEN - + - - + -
Rapa - - + - - +
B
SW480
Glc (mM)
5 (LG)
25 (HG)
Ctrl
NEN
Rapa
Wound healing (%)
40
30
20
10
0
**
***
***
***
HG - - - + + +
NEN - + - - + -
Rapa - - + - - +
C
SW480
Glc (mM)
5 (LG)
25 (HG)
2X
24X
2X
24X
Ctrl
NEN
Rapa
Numbers / mm²
30
20
10
0
***
**
**
HG - - - + + +
NEN - + - - + -
Rapa - - + - - +

Figure 3. The effect of glucose concentration and autophagy activity on focus formation, migration, and sphere formation of CRC cells. A. SW480 cells were treated with 150 nM rapamycin (Rapa) or 1 μM niclosamide ethanolamine (NEN) under 5 or 25 mM glucose medium for 7 days to form foci. The representative images and quantified data of cell-formed foci under 5 mM (low glucose, LG) or 25 mM (high glucose, HG) glucose medium at 7 days were shown. B. To clarify the effect of glucose concentration and autophagy activity on the mobility of SW480 cells, the wound healing assay was conducted. SW480 cells were treated with 1 μM NEN or 150 nM Rapa for 24 h, and the cell migration under 5 or 25 mM glucose conditions were evaluated by the wound healing assay. Representative images of each group at the indicated time points after gap formation were shown. C. To clarify the effect of glucose concentration and autophagy activity on the stemness of SW480 cells, sphere formation assay was conducted. SW480 cells in 5 or 25 mM glucose medium was pretreated with 1 μM NEN or 150 nM Rapa for 24 h to observe sphere formation for 7 days. Quantification is shown in the diagram. Error bars represent mean ± SD. Data were analyzed using one-way ANOVA or two-way ANOVA. * $P<0.05$; **: $P<0.01$; ***: $P<0.001$.

named “niclosamide”, by the Connectivity Map (CMap) platform (https://clue.io/) [47]. Niclosamide is an FDA-approved anthelmintic drug. It has been reported that niclosamide is an mTOR inhibitor and a potential autophagy inducer [46]. NEN (niclosamide ethanolamine), a non-toxic salt form of niclosamide, has higher utility than niclosamide because it can provide high solubility in water, low toxicity, and orally bioavailable *in vivo*. NEN has widely been used to treat digestive system-related cancers [48, 49]. We confirmed that both niclosamide (NC) is autophagy inducers of mouse β-cells (Min-6) and many cancer cell lines [38].

Western blot analysis revealed that high glucose significantly increased the expression of β-catenin, phospho-β-catenin (Ser675), c-Myc, STAT3, phospho-STAT3 (Tyr705), G9a, and cyclin D1, while simultaneously reducing LC3-II levels (**Figure 4A** and **4B**, lane 1 vs. lane 6). These findings suggest that high glucose not only activates tumor-promoting signaling cascades but also suppresses autophagy in CRC cells.

NEN treatment dose-dependently suppressed the levels of β-catenin, p-β-catenin, c-Myc, STAT3, p-STAT3, G9a, and cyclin D1 while increasing LC3-II, key markers of autophagy (**Figure 4A** and **4B**). These effects were observed, and over a time course from 0 to 72 h under the high glucose conditions, where LC3-II levels progressively increased, whereas G9a and other oncogenic proteins diminished by 48-72 h (Figure S5A and S5B). These data support the role of NEN as a potent autophagy inducer and inhibitor of oncogenic signaling in CRC cells.

To further dissect this pathway, pharmacological inhibitors targeting c-Myc, β-catenin, and STAT3 were employed. The c-Myc inhibitor 10058-F4 reduced β-catenin, p-β-catenin, STAT3, p-STAT3, G9a, and cyclin D1 expression, while increasing LC3-II (**Figure 4C**), suggesting that c-Myc lies upstream of both G9a and autophagy suppression. In contrast, the β-catenin inhibitor PNU-74654 decreased STAT3 and p-STAT3 and increased p62 and LC3-II, but did not suppress c-Myc or G9a levels (**Figure 4D**), indicating that β-catenin regulates STAT3 and autophagy independently of c-Myc and G9a. Meanwhile, the STAT3 inhibitor Tanshinone C reduced p-STAT3 without suppressing other key proteins or autophagy markers (β-catenin, c-Myc, G9a, cyclin D1 and LC3-II) (**Figure 4E**), indicating its limited influence in this regulatory network.

To evaluate the role of autophagy more directly, we utilized *Atg5* knockout (SW480-C20) cells. Under high glucose conditions, *Atg5* knockout led to complete loss of LC3-II expression and significantly increased β-catenin, p-β-catenin, and cyclin D1 levels, without altering c-Myc or G9a expression (Figure S6, lane 1 vs. lane 5). Notably, NEN treatment of *Atg5*-deficient cells still reduced β-catenin, p-β-catenin, c-Myc, STAT3, p-STAT3, G9a, and cyclin D1, and increased p62 levels, although LC3-II remained undetectable (Figure S6, lane 5 vs. lane 6). Moreover, compared to wild type SW480, NEN in SW480-C20 cells increased total β-catenin, p62, and cyclinD1 accompanied by the undetectable LC3-II and no evident influence on G9a and c-Myc expression under high glucose conditions (Figure S6, lane 2 vs. lane 6). Silencing G9a decreased G9a level but has no evident effect on β-catenin, p-β-catenin, c-Myc, STAT3, cyclinD1, and LC3-II under high glucose conditions (Figure S6, lane 3 vs. lane 4). Our findings suggest that NEN-induced suppression of the β-catenin - c-Myc - STAT3 -G9a - cyclin D1 axis occurs independently of functional autophagy. Taken together, these results reveal a high glu-

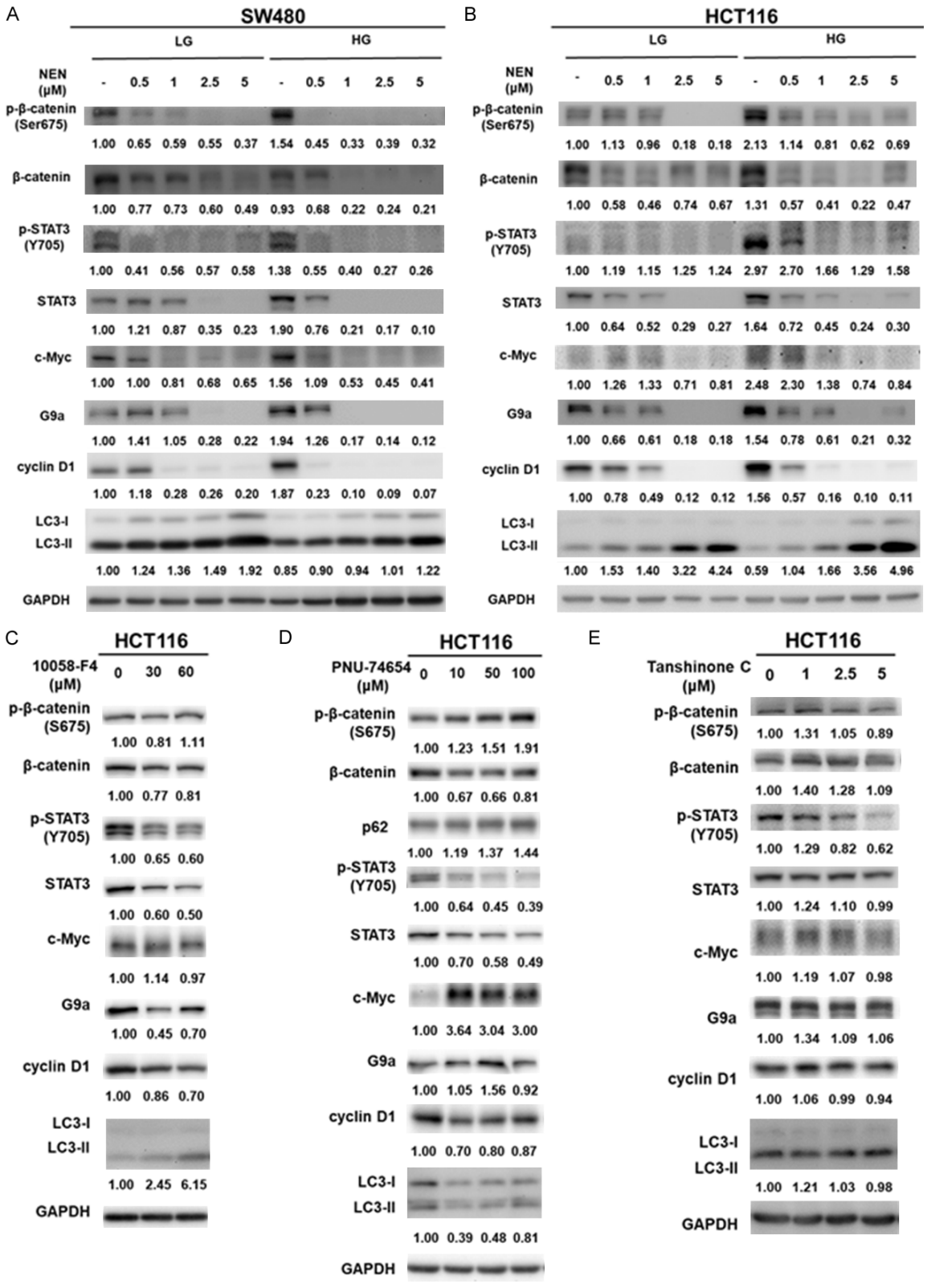

Figure 4. Signaling pathways involved in NEN treatment of CRC cells under low and high glucose conditions. (A) SW480 cells and (B) HCT116 cells maintained in 5 mM (low glucose, LG) or 25 mM (high glucose, HG) glucose medium were treated with various doses of NEN for 24 h. HCT116 cells were treated with (C) c-Myc inhibitor (10058-F4), (D) β-catenin inhibitor (PNU-74654), and (E) STAT3 inhibitor (Tanshinone C) at the indicated doses for 24 h. Protein levels of G9a, β-catenin, phospho-β-catenin (Ser675), p62, STAT3, phospho-STAT3 (Tyr705), c-Myc, cyclin D1, and LC3 were evaluated by Western blotting using specific antibodies. GAPDH was used as the internal control.

cose-induced oncogenic cascade: β-catenin - c-Myc - STAT3 - G9a - cyclin D1 associated with autophagy inhibition in CRC cells. NEN effectively disrupts this cascade and restores the p62-mediated autophagy activity. However, autophagy induction by NEN is mechanistically separable from its suppression of the G9a signaling axis, as demonstrated by the preserved effects of NEN in *Atg5*-deficient cells. These unique events indicate that NEN exerts dual antitumor functions by both inhibiting oncogenic signaling and promoting autophagy, making it a promising candidate for treating high glucose-driven colorectal cancer progression.

Analysis of the expression level of LC3 in clinical CRC specimens as well as the effect of high-fat diet and increased autophagy on tumor formation in xenograft mice

To clarify the autophagy status in CRC patient specimens, we assessed LC3 expression, a marker of autophagy activity, via immunohistochemistry (IHC) on tissue arrays. A total of 14 CRC tissue array slides (61 normal tissues and 209 tumor specimens) were obtained from Kaohsiung Medical University Hospital (Kaohsiung, Taiwan) and National Cheng Kung University Hospital (Tainan, Taiwan) (Table S1). IHC analysis revealed that LC3 expression was significantly higher in CRC tumor tissues compared to adjacent normal tissues (**Figure 5A** and **5B**). Notably, a higher percentage of patients in the non-recurrent group exhibited elevated LC3 levels compared to those in the recurrent group (**Figure 5C**). To further explore clinical correlations, we stratified patients into high- and low-risk groups based on LC3 expression and conducted multivariate analysis using Fisher's exact test. LC3 expression did not show significant association with age, sex, TNM stage, or recurrence status (**Table 1**). These findings suggest that elevated LC3 expression is associated with tumor tissues but reduced recurrence in CRC patients, reflecting the complex and context-dependent role of autophagy in CRC progression. Additionally, LC3 expression appears independent of common clinical factors such as age, sex, TNM stage, and recurrence.

Given the established use of a high-fat diet (HFD) to model obesity and type 2 diabetes in mice [50], we investigated the effect of autophagy modulation in hyperglycemia-associated CRC tumorigenesis. Nude BALB/c mice (7 weeks old) were fed either a chow diet (CD) or HFD for 11 weeks. HFD-fed mice exhibited significantly elevated blood glucose levels compared to CD-fed controls (Figure S7A), though their body weights remained comparable (Figure S7B).

To assess the impact of autophagy in this context, mice were subcutaneously injected with SW480 CRC cells and divided into three groups: (i) CD, (ii) HFD, and (iii) HFD plus the autophagy inducer rapamycin. Three days post-inoculation, rapamycin (3 mg/kg) was administered intraperitoneally every 3 days for 3 weeks. At the endpoint (day 21), tumors were harvested and measured. Tumor volumes were significantly larger in the HFD group than the CD group, whereas rapamycin treatment attenuated tumor growth in HFD-fed mice (**Figure 5D**).

Western blot analysis of tumor tissues showed reduced LC3-II levels in HFD tumors compared to CD controls, while rapamycin restored LC3-II levels in the HFD group (**Figure 5E**, lane 3 vs. lanes 2). IHC analysis confirmed increased Ki67 expression, a marker of proliferation, in HFD tumors, which was reduced by rapamycin treatment (**Figure 5F**). Similarly, LC3-II expression decreased in the HFD group but was elevated upon rapamycin treatment (**Figure 5F**). Previously, we demonstrated that secretory autophagy facilitates RAB37-mediated insulin secretion to maintain insulin/glucose homeostasis [38]. In line with this, serum insulin levels were elevated in HFD-fed mice and further increased following rapamycin administration (Figure S7C). These findings suggest that a high-fat diet promotes CRC tumor growth by suppressing autophagy, as indicated by reduced LC3-II levels and increased proliferation. Induction of autophagy with rapamycin restores LC3-II expression, reduces tumor growth and Ki67 levels, and enhances insulin secretion, highlighting the protective role of autophagy in hyperglycemia-driven tumor progression.

Discussion

In this study, we demonstrate that (1) high glucose suppresses autophagy in CRC cells, as evidenced by decreased LC3-II levels, which is accompanied by enhanced tumor cell viability, colony formation, motility, and mice tumor for-

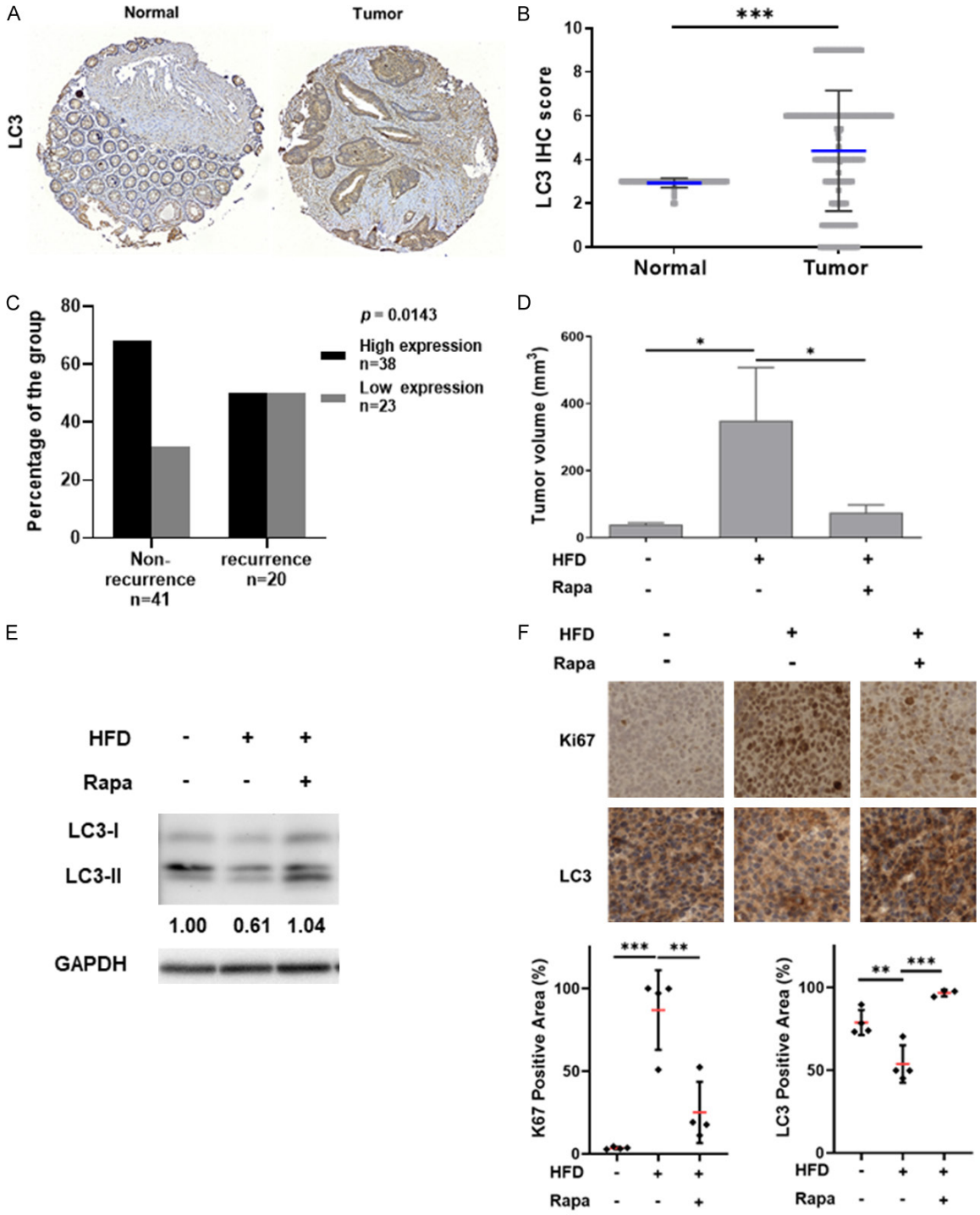

Figure 5. Analysis of the expression level of LC3 in clinical CRC specimens as well as the effect of high-fat diet and increased autophagy on tumor formation in xenograft mice. A. Representative images of LC3 expression in the tumor and the normal tissue of CRC specimens in the tissue array. B. Quantification of LC3 protein levels in non-tumor (n=59) and tumor (n=169) sections of CRC specimens. The level of LC3 expression was scored from 0 to +9 by a pathologist. A paired t-test was used to compare two groups. Error bars represent mean ± SD. Data were analyzed by Student's t-test. ***: $P<0.001$. C. Percentage of high and low LC3 expression in non-recurrence (n=41) and recurrence (n=20) CRC specimens. High and low LC3 protein expression was defined by the mean IHC value of the tumor tissue. Data were analyzed using Fisher's exact test. D. SW480 cells (2×10^6) were inoculated subcutaneously into nude mice fed with HFD for 11 weeks. Three days after cancer cell inoculation, rapamycin (Rapa, 3 mg/kg) was intraperitoneally injected into the mice every 3 days for 21 days and sacrificed. The final tumor volume was

determined. E. The protein expression level was evaluated by Western blotting using an anti-LC3 antibody. GAPDH was used as the internal control. F. Representative Ki67 and LC3 IHC staining images showed the protein expression levels in the tumor tissues. Magnification: 20×. The quantification was based on the average of 4 randomly selected fields. The values shown are expressed as the mean ± SD. Data were analyzed using one-way ANOVA. ns: no significant; *P<0.05; **P<0.01; ***P<0.001.

Table 1. Correlation of LC3 protein level with clinical multiple-parameters of the CRC patients

Parameters	LC3		*P* value#
	Low@ (Number)	High@ (Number)	
Gender			
Male	51	73	0.7763
Female	37	48	
Age (years)			
<66	49	55	0.1264
≥66	39	66	
TNM stage			
Stage 1-2	43	74	0.0908
Stage 3-4	45	47	

1. The definitions of gender, age, and TNM stage are the same as in Table S1. @: The LC3 IHC score is higher than the IHC mean value of the tumor tissue, defined as High; the others are Low. #: Fisher's exact test was used for multiple-factor analysis.

mation (**Figures 1A-C**, **3A**, **3B** and **5D**). Interestingly, while high glucose impairs autophagy and promotes cancer cell development, analysis of patient specimens revealed that elevated autophagy marker LC3 protein are detected in CRC tumors (**Figure 5A** and **5B**), underscoring the microenvironment-dependent roles of autophagy in CRC progression. This discrepancy is consistent with the notion that autophagy plays dual roles during cancer development, initially suppressing and later supporting tumor progression [51]. (2) Pharmacological induction of autophagy using inducers increased autophagic activity and suppresses CRC progression (**Figures 2** and **5D**), while also enhancing sensitivity to chemotherapeutic agents such as 5-fluorouracil (5-FU) and oxaliplatin (Oxa) under high glucose conditions (**Figure 2G-J**). These effects are reversed by *Atg5* silencing, but not knockout, confirming the functional significance and complexity of autophagy in mediating therapeutic response under high glucose environments (Figures S1 and S3). (3) Mechanistically, we identify G9a as a downstream effector of high glucose-induced c-Myc activity (**Figure 4C**), contributing to tumorigenic phenotypes via upregulation of STAT3, β-catenin, and cyclin D1 (**Figures 4A**, **4B** and **6A**). Our data show that NEN, by increasing autophagy, also downregulates c-Myc, STAT3, G9a, and β-catenin, thereby reducing CRC tumorigenesis (**Figures 4A**, **4B** and **6B**). This is consistent with prior reports that niclosamide targets multiple oncogenic signaling pathways including Wnt/β-catenin, NF-κB, STAT3, mTORC1, and p53 to suppress c-Myc expression and function [52-55]. In this study, we observed elevated blood glucose levels in a high-fat diet mouse model. Administration of the autophagy inducer rapamycin to mice bearing CRC SW480 xenografts resulted in increased systemic insulin levels (Figure S7C) and a concomitant reduction in tumor burden (**Figure 5D-F**). These findings support our hypothesis that autophagy differentially contributes to physiological processes: secretory autophagy enhances systemic insulin secretion, thereby influencing glucose homeostasis, while degradative autophagy plays a crucial role in suppressing tumor formation. Specifically, rapamycin-induced autophagy in a hyperglycemic CRC xenograft model demonstrably increased insulin secretion, corroborating our prior observations regarding Rab37-mediated secretory autophagy's regulation of glucose homeostasis both *in vitro* and *in vivo* [38]. Meanwhile, NEN accompanied by induced degradative autophagy inhibited high glucose-related oncogenic regulators such as G9a, β-catenin, and c-Myc, thereby suppressing tumorigenesis (**Figures 4** and **6**). Although previous studies suggested that G9a negatively regulates autophagy [56], our results reveal that in CRC cells under high glucose conditions, G9a and autophagy may function in parallel rather than through a reciprocal regulatory loop (**Figures 6** and S6), suggesting a combinatorial therapeutic strategy.

The paradoxical role of autophagy in CRC - tumor-suppressive under certain conditions yet tumor-supportive in others - is consistent with Levine's (2007) comment that autophagy plays dual roles during cancer development [51].

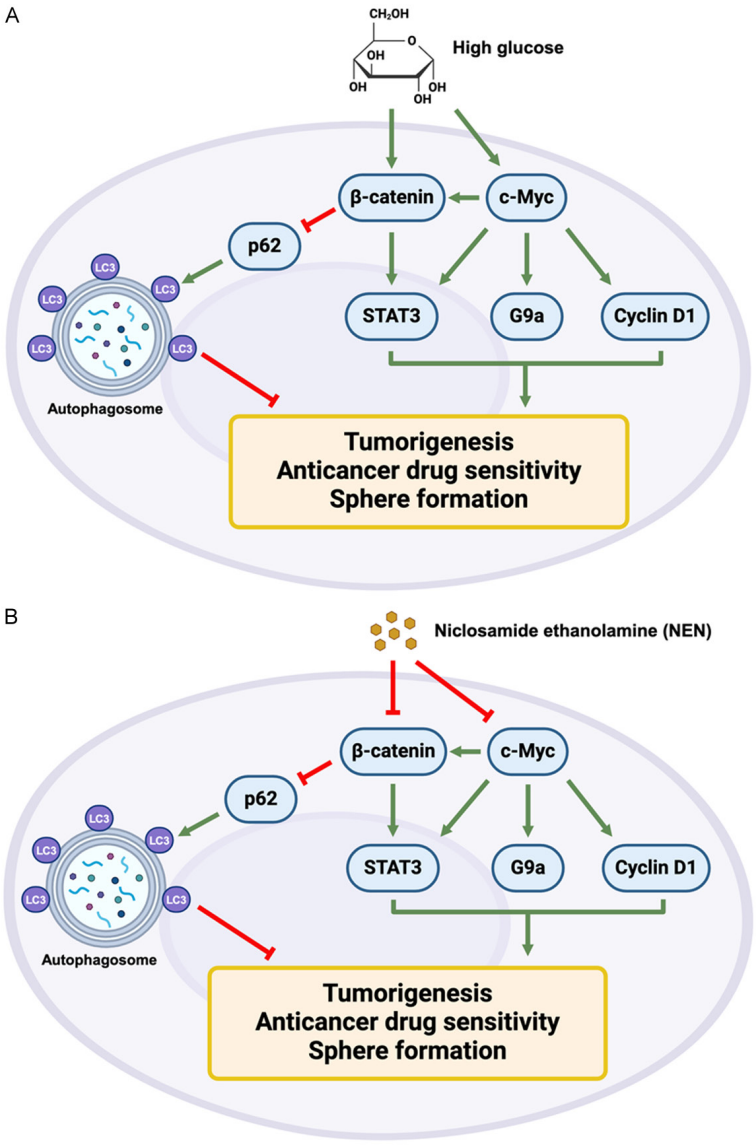

Figure 6. High glucose and NEN treatment related signaling pathways involved in CRC tumorigenesis. A. High glucose induces β-catenin - c-Myc - STAT3 - G9a - cyclin D1 signaling together with decreased autophagy. B. NEN decreases β-catenin - c-Myc - STAT3 - G9a - cyclin D1 axis accompanied by increased autophagy Green line: induction signaling; Red line: suppression signaling. These images were created in https://BioRender.com.

Briefly, early-stage autophagy suppresses tumorigenesis by removing damaged organelles and maintaining homeostasis, whereas later stages autophagy facilitates survival in stress-resistant cancer cells. Our observation that CRC tumor tissues exhibit elevated LC3 levels yet high glucose reduces LC3-II *in vitro* is consistent with Levine's speculation that autophagy status is temporally and spatially regulated during cancer development under various conditions. In this study, our finding that high glucose suppresses autophagy activity is consistent with Li *et al.*'s report that high glucose suppresses autophagy through induction of PI3K/Akt/mTOR axis in CRC tumorigenesis [57]. Similarly, Zhou *et al.* (2019) reported that high blood glucose decreases autophagy and promotes pancreatic cancer through SREBP1 [58]. However, the status of autophagy activity at late stages of hyperglycemic tumors remains to be determined. In conclusion, regardless the variation of autophagy status in cancers, we demonstrate that further induction of autophagy activity by inducers results in cancer cell death and mitigation of malignant transformation of cancer cells through autophagy-related excessive degradation.

Moreover, Cheng *et al.* (2021) [59] reveal that hyperglycemia-related recurrence and drug resistance in CRC are epigenetically regulated. Altogether, above findings corroborate and reinforce our evidence that c-Myc-mediated G9a transcription plays a central role in CRC cells under high glucose conditions (**Figure 6A**).

Ichikawa *et al.* (2022) [60] showed that silencing G9a increases CRC sphere formation through IL-8 upregulation, contrasting with our findings where G9a suppression by NEN or Rapa reduced sphere formation (**Figure 3C**). Moreover, Sato *et al.* (2020) [30] reported that high glucose enhances pancreatic cancer sphere formation via p-STAT3 and c-Myc related pathways. In our CRC model, however, high glucose suppressed sphere formation (**Figure 3C**), even in the presence of upregulated p-STAT3 and c-Myc (**Figure 4A** and **4B**), highlighting potential tissue-specific responses. Altogether, these discrepancies may arise from differen-

tial experimental systems, levels of G9a silencing, or cancer subtype-specific epigenetic programs.

Yamazaki *et al.* (2020) [61] demonstrated that loss of autophagy genes sensitizes mammary carcinoma cells to radiation, echoing our findings that *Atg5* silencing increases CRC chemosensitivity under specific conditions (Figure S3). Notably, the duality of *Atg5*-tumor suppressive in autophagy-competent states, yet tumor-promoting under autophagy-deficient settings-has been similarly proposed [62].

Niclosamide's diverse anti-cancer effects have been attributed to its ability to target multiple upstream regulators of c-Myc, including Wnt/β-catenin, NF-κB, STAT3, mTORC1, and AMPK pathways [52, 53]. Niclosamide may also post-translationally regulate c-Myc via GSK-3β and PP2A [54, 55]. Our results support these observations by demonstrating that NEN downregulates β-catenin, c-Myc, STAT3, G9a, and cyclin D1 protein levels (**Figures 4** and **6B**).

Finally, previous work by our group and others has shown that autophagy inducers can improve insulin secretion and glycemic control [38], extending the implications of autophagy modulation beyond cancer cell-intrinsic effects to systemic metabolic benefits.

This study makes several important contributions to the field of cancer biology and therapy: (1) clarifying the role of autophagy under metabolic stress, we address a previously unresolved paradox regarding autophagy status in CRC tumors versus cultured CRC cells. By demonstrating that high glucose suppresses autophagy and promotes CRC progression, while patient tumors show elevated autophagy markers, we propose a model of metabolic adaptation where autophagy levels are possibly modulated according to systemic and microenvironmental cues; (2) therapeutic potential of autophagy inducers in hyperglycemic CRC, we establish that pharmacological induction of autophagy via rapamycin or NEN suppresses CRC viability, focus formation, migration, tumor formation, and enhances sensitivity to standard chemotherapeutics; (3) G9a as a downstream target of c-Myc in high glucose-driven CRC progression, we identify c-Myc as a key transcriptional activator of G9a under high glucose, providing mechanistic insight into how metabolic stress promotes epigenetic reprogramming; (4) no reciprocal regulation between autophagy and G9a; contrary to some reports, we found that increasing autophagy activity did not alter G9a expression levels, and vice versa. This indicates that autophagy and G9a pathways independently converge on common tumorigenesis, and could be targeted simultaneously without cross-inhibition.

Despite the strengths of this study, several limitations warrant consideration: The dual nature of autophagy complicates its therapeutic modulation. Although we show consistent tumor suppression with autophagy inducers in our models, the long-term consequences of sustained autophagy activation especially *in vivo* remain unclear and warrant further investigation.

While we demonstrate that G9a expression is regulated by c-Myc and contributes to tumorigenesis, future studies using ChIP-seq and transcriptomic profiling are necessary to identify the target genes epigenetically regulated by G9a under hyperglycemic conditions. Because others have reported that G9a's targets related to cancer cell malignancy are often through the silencing of tumor suppressor genes or activation of oncogenic pathways by H3K9 methylation, or even through methylation of non-histone proteins like p53 [63]. Moreover, we have reported that G9a governs chemoradioresistance in colon cancer. Knockdown of G9a increases the sensitivity of CRC cells to radiation and DNA damaging agents through the PP2A-RPA axis [56]. Nevertheless, we conducted a preliminary experiment to screen for the target of G9a using H3K9m2 antibody-immunoprecipitation followed by ChIP analysis, our data showed that in AGS cells G9a-related H3K9m2 antibody binds to the promoter of *Atg7* and *Beclin1* genes. After NEN treatment resulted in significant decrease binding of H3K9m2 with *Atg7* an *Beclin1*, (unpublished data) which is consistent with the induction of autophagy activity.

The discrepant effects of *Atg5* silencing and knockout on SW480 (Figure S1D, S1E) as well as *Atg5* silencing on SW480 versus HCT116 cells (Figure S1D, S1F) may be caused by the following reasons: 1) for the former in SW480 cells, may be related to off-label targeting of *Atg5* silencing or the degree of suppression by

Table 2. Genetic background of five oncogenic genes in CRC SW480 and HCT116 cell lines

Cell line	KRAS	BRAF	PIK3CA	PTEN	TP53
SW480	G12V	wild type	wild type	wild type	R273H P309S
HCT116	G13D	wild type	H1047R	wild type	wild type

silencing or knockout *Atg5* genes within the cell; 2) for the latter, may stem from their distinct genetic backgrounds (**Table 2**) [64]. Understanding how genetic mutations (e.g., TP53, KRAS, PIK3CA, BRAF, PTEN) influence autophagy response may be helpful for patient stratification and precision therapy.

While our mouse xenograft data support the therapeutic efficacy of autophagy inducers, clinical relevance needs validation. Studies involving patient-derived organoids, orthotopic tumor models, and metabolic profiling in CRC patients are essential next steps.

Although we observed no reciprocal inhibition between G9a and autophagy, other studies suggest bidirectional regulation. The exact molecular mechanisms underlying the independence or interaction of these pathways need further exploration, potentially through proteomics or CRISPR-based genetic screens.

In conclusion, this study provides compelling evidence that autophagy induction under hyperglycemic conditions mitigates CRC progression and enhances therapeutic efficacy. By elucidating the mechanistic role of c-Myc-G9a signaling and demonstrating the effects of autophagy, we propose a novel therapeutic strategy that integrates metabolic regulation with cancer control. Future research should aim to dissect the epigenetic landscape governed by G9a and refine autophagy-based interventions for clinical application.

Acknowledgements

The authors thank the Center for Laboratory Animals in Kaohsiung Medical University for the animal care. The authors thank the Center for Research Resources and Development in Kaohsiung Medical University for the assistance in TissueFAXS and confocal image analysis. This study was supported by the grants from National Science and Technology Council, Taiwan [NSTC-113-2320-B-037-002-, NSTC 114-2314-B-037-103-MY3, NSTC 114-2321-B-037-003], Kaohsiung Medical University Hospital Grant [KMUH113-3R31], Kaohsiung Medical University Research Center Grant [KMU-TC113A04, and KMU-TC114A04].

Disclosure of conflict of interest

The authors declare that the research was conducted in the absence of any commercial or financial relationships that could be construed as a potential conflict of interest.

Abbreviations

5-FU, 5-fluorouracil; ATGs, autophagy-related genes; CD, control diet; COAD, colon adenocarcinoma; CRC, colorectal cancer; EHMT2/G9a, euchromatic histone-lysine N-methyltransferase 2; Glc, Glucose; HG, high glucose; HFD, high-fat diet; LG, low glucose; NEN, niclosamide ethanolamine salt; Oxa, oxaliplatin; Rapa, rapamycin.

Address correspondence to: Dr. Hsiao-Sheng Liu, M.Sc. Program in Tropical Medicine, Kaohsiung Medical University, No. 100, Shiquan 1st Rd., Sanmin Dist., Kaohsiung 807378, Taiwan. Tel: +886-7-3121101 Ext. 2378; E-mail: hsliu713@kmu.edu.tw; Dr. Ying-Ray Lee, Department of Microbiology and Immunology, Kaohsiung Medical University, No. 100, Shiquan 1st Rd., Sanmin Dist., Kaohsiung 807378, Taiwan. Tel: +886-7-3121101 Ext. 2150#12; E-mail: yingray.lee@gmail.com; Dr. Jaw-Yuan Wang, Division of Colorectal Surgery, Department of Surgery, Kaohsiung Medical University Hospital, Kaohsiung Medical University, No. 100, Shiquan 1st Rd., Sanmin Dist., Kaohsiung 807378, Taiwan. Tel: +886-7-3121101; E-mail: cy614112@ms14.hinet.net; Jawyuanwang@gmail.com

References

[1] Purandare NC, Dua SG, Arora A, Shah S and Rangarajan V. Colorectal cancer-patterns of locoregional recurrence and distant metastases as demonstrated by FDG PET/CT. Indian J Radiol Imaging 2010; 20: 284-288.

[2] Wang B, Wang S, Wang W, Liu E, Guo S, Zhao C, Niu J and Zhang Z. Hyperglycemia promotes

liver metastasis of colorectal cancer via upregulation of integrin αvβ6. Med Sci Monit 2021; 27: e930921.
[3] Xia B, He Q, Pan Y, Gao F, Liu A, Tang Y, Chong C, Teoh AYB, Li F, He Y, Zhang C and Yuan J. Metabolic syndrome and risk of pancreatic cancer: a population-based prospective cohort study. Int J Cancer 2020; 147: 3384-3393.
[4] Montemurro N, Perrini P and Rapone B. Clinical risk and overall survival in patients with diabetes mellitus, hyperglycemia and glioblastoma multiforme. A review of the current literature. Int J Environ Res Public Health 2020; 17: 8501.
[5] Yang IP, Miao ZF, Huang CW, Tsai HL, Yeh YS, Su WC, Chang TK, Chang SF and Wang JY. High blood sugar levels but not diabetes mellitus significantly enhance oxaliplatin chemoresistance in patients with stage III colorectal cancer receiving adjuvant FOLFOX6 chemotherapy. Ther Adv Med Oncol 2019; 11: 1758835919866964.
[6] Li J, Liu J, Gao C, Liu F and Zhao H. Increased mortality for colorectal cancer patients with preexisting diabetes mellitus: an updated meta-analysis. Oncotarget 2017; 8: 62478-62488.
[7] Ávalos Y, Canales J, Bravo-Sagua R, Criollo A, Lavandero S and Quest AF. Tumor suppression and promotion by autophagy. Biomed Res Int 2014; 2014: 603980.
[8] Kisen GØ, Tessitore L, Costelli P, Gordon PB, Schwarze PE, Baccino FM and Seglen PO. Reduced autophagic activity in primary rat hepatocellular carcinoma and ascites hepatoma cells. Carcinogenesis 1993; 14: 2501-2505.
[9] Cheng WM, Li PC, Nguyen MT, Lin YT, Huang YT, Cheng TS, Nguyen TH, Tran TH, Huang TY, Hoang TH, Chen SY, Chu YC, Wu CW, Lee MF, Chiou YS, Liu HS, Hong YR, Chang PM, Hu YF, Chang YC, Lai JM and Huang CF. Repurposing pitavastatin and atorvastatin to overcome chemoresistance of metastatic colorectal cancer under high glucose conditions. Cancer Cell Int 2025; 25: 79.
[10] Jeong S, Kim BG, Kim DY, Kim BR, Kim JL, Park SH, Na YJ, Jo MJ, Yun HK, Jeong YA, Kim HJ, Lee SI, Kim HD, Kim DH, Oh SC and Lee DH. Cannabidiol overcomes oxaliplatin resistance by enhancing NOS3- and SOD2-induced autophagy in human colorectal cancer cells. Cancers (Basel) 2019; 11: 781.
[11] Chu CA, Lee CT, Lee JC, Wang YW, Huang CT, Lan SH, Lin PC, Lin BW, Tian YF, Liu HS and Chow NH. MiR-338-5p promotes metastasis of colorectal cancer by inhibition of phosphatidylinositol 3-kinase, catalytic subunit type 3-mediated autophagy pathway. EBioMedicine 2019; 43: 270-281.
[12] Wilson CM, Magnaudeix A, Yardin C and Terro F. Autophagy dysfunction and its link to Alzheimer's disease and type II diabetes mellitus. CNS Neurol Disord Drug Targets 2014; 13: 226-246.
[13] Ouyang C, You J and Xie Z. The interplay between autophagy and apoptosis in the diabetic heart. J Mol Cell Cardiol 2014; 71: 71-80.
[14] Wang Y, Li YB, Yin JJ, Wang Y, Zhu LB, Xie GY and Pan SH. Autophagy regulates inflammation following oxidative injury in diabetes. Autophagy 2013; 9: 272-277.
[15] Chen Z, Li Y, Zhang C, Yi H, Wu C, Wang J, Liu Y, Tan J and Wen J. Downregulation of Beclin 1 and impairment of autophagy in a small population of colorectal cancer. Dig Dis Sci 2013; 58: 2887-2894.
[16] Ezaki J, Matsumoto N, Takeda-Ezaki M, Komatsu M, Takahashi K, Hiraoka Y, Taka H, Fujimura T, Takehana K, Yoshida M, Iwata J, Tanida I, Furuya N, Zheng DM, Tada N, Tanaka K, Kominami E and Ueno T. Liver autophagy contributes to the maintenance of blood glucose and amino acid levels. Autophagy 2011; 7: 727-736.
[17] Wu SY, Lan SH and Liu HS. Degradative autophagy selectively regulates CCND1 (cyclin D1) and MIR224, two oncogenic factors involved in hepatocellular carcinoma tumorigenesis. Autophagy 2019; 15: 729-730.
[18] New J and Thomas SM. Autophagy-dependent secretion: mechanism, factors secreted, and disease implications. Autophagy 2019; 15: 1682-1693.
[19] Wu SY, Lan SH, Wu SR, Chiu YC, Lin XZ, Su IJ, Tsai TF, Yen CJ, Lu TH, Liang FW, Li CY, Su HJ, Su CL and Liu HS. Hepatocellular carcinoma-related cyclin D1 is selectively regulated by autophagy degradation system. Hepatology 2018; 68: 141-154.
[20] Deretic V, Jiang S and Dupont N. Autophagy intersections with conventional and unconventional secretion in tissue development, remodeling and inflammation. Trends Cell Biol 2012; 22: 397-406.
[21] Wu SY, Lan SH, Cheng DE, Chen WK, Shen CH, Lee YR, Zuchini R and Liu HS. Ras-related tumorigenesis is suppressed by BNIP3-mediated autophagy through inhibition of cell proliferation. Neoplasia 2011; 13: 1171-1182.
[22] Gulhati P, Cai Q, Li J, Liu J, Rychahou PG, Qiu S, Lee EY, Silva SR, Bowen KA, Gao T and Evers BM. Targeted inhibition of mammalian target of rapamycin signaling inhibits tumorigenesis of colorectal cancer. Clin Cancer Res 2009; 15: 7207-7216.
[23] Jeong S, Kim DY, Kang SH, Yun HK, Kim JL, Kim BR, Park SH, Na YJ, Jo MJ, Jeong YA, Kim BG, Lee DH and Oh SC. Docosahexaenoic acid en-

hances oxaliplatin-induced autophagic cell death via the ER stress/Sesn2 pathway in colorectal cancer. Cancers (Basel) 2019; 11: 982.
[24] Hama Y, Ogasawara Y and Noda NN. Autophagy and cancer: basic mechanisms and inhibitor development. Cancer Sci 2023; 114: 2699-2708.
[25] Jalali P, Shahmoradi A, Samii A, Mazloomnejad R, Hatamnejad MR, Saeed A, Namdar A and Salehi Z. The role of autophagy in cancer: from molecular mechanism to therapeutic window. Front Immunol 2025; 16: 1528230.
[26] Galluzzi L, Pietrocola F, Bravo-San Pedro JM, Amaravadi RK, Baehrecke EH, Cecconi F, Codogno P, Debnath J, Gewirtz DA, Karantza V, Kimmelman A, Kumar S, Levine B, Maiuri MC, Martin SJ, Penninger J, Piacentini M, Rubinsztein DC, Simon HU, Simonsen A, Thorburn AM, Velasco G, Ryan KM and Kroemer G. Autophagy in malignant transformation and cancer progression. EMBO J 2015; 34: 856-880.
[27] Rodrigues Mantuano N, Stanczak MA, Oliveira IA, Kirchhammer N, Filardy AA, Monaco G, Santos RC, Fonseca AC, Fontes M, Bastos CS Jr, Dias WB, Zippelius A, Todeschini AR and Läubli H. Hyperglycemia enhances cancer immune evasion by inducing alternative macrophage polarization through increased O-GlcNAcylation. Cancer Immunol Res 2020; 8: 1262-1272.
[28] Vasconcelos-Dos-Santos A, Loponte HF, Mantuano NR, Oliveira IA, de Paula IF, Teixeira LK, de-Freitas-Junior JC, Gondim KC, Heise N, Mohana-Borges R, Morgado-Díaz JA, Dias WB and Todeschini AR. Hyperglycemia exacerbates colon cancer malignancy through hexosamine biosynthetic pathway. Oncogenesis 2017; 6: e306.
[29] Quagliariello V, De Laurentiis M, Cocco S, Rea G, Bonelli A, Caronna A, Lombari MC, Conforti G, Berretta M, Botti G and Maurea N. NLRP3 as putative marker of ipilimumab-induced cardiotoxicity in the presence of hyperglycemia in estrogen-responsive and triple-negative breast cancer cells. Int J Mol Sci 2020; 21: 7802.
[30] Sato K, Hikita H, Myojin Y, Fukumoto K, Murai K, Sakane S, Tamura T, Yamai T, Nozaki Y, Yoshioka T, Kodama T, Shigekawa M, Sakamori R, Tatsumi T and Takehara T. Hyperglycemia enhances pancreatic cancer progression accompanied by elevations in phosphorylated STAT3 and MYC levels. PLoS One 2020; 15: e0235573.
[31] Franko A, Berti L, Hennenlotter J, Rausch S, Scharpf MO, Angelis MH, Stenzl A, Peter A, Birkenfeld AL, Lutz SZ, Häring HU and Heni M. Increased expressions of matrix metalloproteinases (MMPs) in prostate cancer tissues of men with type 2 diabetes. Biomedicines 2020; 8: 507.
[32] Cao YP, Sun JY, Li MQ, Dong Y, Zhang YH, Yan J, Huang RM and Yan X. Inhibition of G9a by a small molecule inhibitor, UNC0642, induces apoptosis of human bladder cancer cells. Acta Pharmacol Sin 2019; 40: 1076-1084.
[33] Zhao H and Wu K. Effect of hyperglycemia on the occurrence and prognosis of colorectal cancer. Am J Transl Res 2024; 16: 2070-2081.
[34] Zintzaras E, Miligkos M, Ziakas P, Balk EM, Mademtzoglou D, Doxani C, Mprotsis T, Gowri R, Xanthopoulou P, Mpoulimari I, Kokkali C, Dimoulou G, Rodopolou P, Stefanidis I, Kent DM and Hadjigeorgiou GM. Assessment of the relative effectiveness and tolerability of treatments of type 2 diabetes mellitus: a network meta-analysis. Clin Ther 2014; 36: 1443-1453, e9.
[35] Mazza S and Maffucci T. Autophagy and pancreatic β-cells. Vitam Horm 2014; 95: 145-164.
[36] Quan W, Lim YM and Lee MS. Role of autophagy in diabetes and endoplasmic reticulum stress of pancreatic β-cells. Exp Mol Med 2012; 44: 81-88.
[37] Jung HS, Chung KW, Won Kim J, Kim J, Komatsu M, Tanaka K, Nguyen YH, Kang TM, Yoon KH, Kim JW, Jeong YT, Han MS, Lee MK, Kim KW, Shin J and Lee MS. Loss of autophagy diminishes pancreatic β cell mass and function with resultant hyperglycemia. Cell Metab 2008; 8: 318-324.
[38] Wu SY, Wu HT, Wang YC, Chang CJ, Shan YS, Wu SR, Chiu YC, Hsu CL, Juan HF, Lan KY, Chu CW, Lee YR, Lan SH and Liu HS. Secretory autophagy promotes RAB37-mediated insulin secretion under glucose stimulation both in vitro and in vivo. Autophagy 2023; 19: 1239-1257.
[39] Chun Y and Kim J. Autophagy: an essential degradation program for cellular homeostasis and life. Cells 2018; 7: 278.
[40] Jiang X, Overholtzer M and Thompson CB. Autophagy in cellular metabolism and cancer. J Clin Invest 2015; 125: 47-54.
[41] Goginashvili A, Zhang Z, Erbs E, Spiegelhalter C, Kessler P, Mihlan M, Pasquier A, Krupina K, Schieber N, Cinque L, Morvan J, Sumara I, Schwab Y, Settembre C and Ricci R. Insulin granules. Insulin secretory granules control autophagy in pancreatic β cells. Science 2015; 347: 878-882.
[42] Jakubek P, Pakula B, Rossmeisl M, Pinton P, Rimessi A and Wieckowski MR. Autophagy alterations in obesity, type 2 diabetes, and metabolic dysfunction-associated steatotic liver disease: the evidence from human studies. Intern Emerg Med 2024; 19: 1473-1491.

[43] Guo Y, Lin C, Xu P, Wu S, Fu X, Xia W and Yao M. AGEs induced autophagy impairs cutaneous wound healing via stimulating macrophage polarization to M1 in diabetes. Sci Rep 2016; 6: 36416.
[44] Chen J, Ren Y, Gui C, Zhao M, Wu X, Mao K, Li W and Zou F. Phosphorylation of Parkin at serine 131 by p38 MAPK promotes mitochondrial dysfunction and neuronal death in mutant A53T α-synuclein model of Parkinson's disease. Cell Death Dis 2018; 9: 700.
[45] Van Heek M, Compton DS, France CF, Tedesco RP, Fawzi AB, Graziano MP, Sybertz EJ, Strader CD and Davis HR Jr. Diet-induced obese mice develop peripheral, but not central, resistance to leptin. J Clin Invest 1997; 99: 385-390.
[46] Balgi AD, Fonseca BD, Donohue E, Tsang TC, Lajoie P, Proud CG, Nabi IR and Roberge M. Screen for chemical modulators of autophagy reveals novel therapeutic inhibitors of mTORC1 signaling. PLoS One 2009; 4: e7124.
[47] Kubicek S, O'Sullivan RJ, August EM, Hickey ER, Zhang Q, Teodoro ML, Rea S, Mechtler K, Kowalski JA, Homon CA, Kelly TA and Jenuwein T. Reversal of H3K9me2 by a small-molecule inhibitor for the G9a histone methyltransferase. Mol Cell 2007; 25: 473-481.
[48] Wang Z, Ren J, Du J, Wang H, Liu J and Wang G. Niclosamide as a promising therapeutic player in human cancer and other diseases. Int J Mol Sci 2022; 23: 16116.
[49] Alasadi A, Chen M, Swapna GVT, Tao H, Guo J, Collantes J, Fadhil N, Montelione GT and Jin S. Effect of mitochondrial uncouplers niclosamide ethanolamine (NEN) and oxyclozanide on hepatic metastasis of colon cancer. Cell Death Dis 2018; 9: 215.
[50] Muthulakshmi S, Chakrabarti AK and Mukherjee S. Gene expression profile of high-fat diet-fed C57BL/6J mice: in search of potential role of azelaic acid. J Physiol Biochem 2015; 71: 29-42.
[51] Levine B. Cell biology: autophagy and cancer. Nature 2007; 446: 745-747.
[52] Wiggins R, Woo J and Mito S. Optimizing niclosamide for cancer therapy: improving bioavailability via structural modification and nanotechnology. Cancers (Basel) 2024; 16: 3548.
[53] Jiang H, Li AM and Ye J. The magic bullet: niclosamide. Front Oncol 2022; 12: 1004978.
[54] Gregory MA, Qi Y and Hann SR. Phosphorylation by glycogen synthase kinase-3 controls c-myc proteolysis and subnuclear localization. J Biol Chem 2003; 278: 51606-51612.
[55] Kim MO, Choe MH, Yoon YN, Ahn J, Yoo M, Jung KY, An S, Hwang SG, Oh JS and Kim JS. Antihelminthic drug niclosamide inhibits CIP2A and reactivates tumor suppressor protein phosphatase 2A in non-small cell lung cancer cells. Biochem Pharmacol 2017; 144: 78-89.
[56] Luo CW, Wang JY, Hung WC, Peng G, Tsai YL, Chang TM, Chai CY, Lin CH and Pan MR. G9a governs colon cancer stem cell phenotype and chemoradioresistance through PP2A-RPA axis-mediated DNA damage response. Radiother Oncol 2017; 124: 395-402.
[57] Li F, Wan X, Li Z and Zhou L. High glucose inhibits autophagy and promotes the proliferation and metastasis of colorectal cancer through the PI3K/AKT/mTOR pathway. Cancer Med 2024; 13: e7382.
[58] Zhou C, Qian W, Li J, Ma J, Chen X, Jiang Z, Cheng L, Duan W, Wang Z, Wu Z, Ma Q and Li X. High glucose microenvironment accelerates tumor growth via SREBP1-autophagy axis in pancreatic cancer. J Exp Clin Cancer Res 2019; 38: 302.
[59] Cheng HC, Chang TK, Su WC, Tsai HL and Wang JY. Narrative review of the influence of diabetes mellitus and hyperglycemia on colorectal cancer risk and oncological outcomes. Transl Oncol 2021; 14: 101089.
[60] Ichikawa Y, Takahashi H, Chinen Y, Arita A, Sekido Y, Hata T, Ogino T, Miyoshi N, Uemura M, Yamamoto H, Mizushima T, Doki Y and Eguchi H. Low G9a expression is a tumor progression factor of colorectal cancer via IL-8 promotion. Carcinogenesis 2022; 43: 797-807.
[61] Yamazaki T, Kirchmair A, Sato A, Buqué A, Rybstein M, Petroni G, Bloy N, Finotello F, Stafford L, Navarro Manzano E, Ayala de la Peña F, García-Martínez E, Formenti SC, Trajanoski Z and Galluzzi L. Mitochondrial DNA drives abscopal responses to radiation that are inhibited by autophagy. Nat Immunol 2020; 21: 1160-1171.
[62] Liu HS, Wang YP, Lin PW, Chu ML, Lan SH, Wu SY, Lee YR and Chang HY. The role of Atg5 gene in tumorigenesis under autophagy deficiency conditions. Kaohsiung J Med Sci 2024; 40: 631-641.
[63] Ni Y, Shi M, Liu L, Lin D, Zeng H, Ong C and Wang Y. G9a in cancer: mechanisms, therapeutic advancements, and clinical implications. Cancers (Basel) 2024; 16: 2175.
[64] Ahmed D, Eide PW, Eilertsen IA, Danielsen SA, Eknæs M, Hektoen M, Lind GE and Lothe RA. Epigenetic and genetic features of 24 colon cancer cell lines. Oncogenesis 2013; 2: e71.

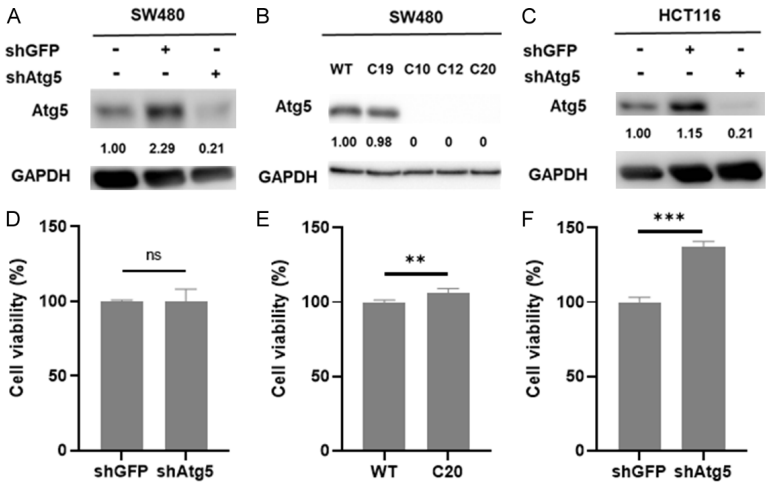

Figure S1. The effect of silencing Atg5 gene on the viability of CRC cell lines under high glucose conditions. (A, D) SW480 cells and (C, F) HCT116 cells were treated with lentiviral shRNA to silence the Atg5 gene. (B, E) SW480 cells were cloned by CRISPR-Cas9 knockout *Atg5* gene. SW480-C19 was the heterologous recombination, and the others (SW480-C10, C12, C20) were the homologous recombination. (A-C) Atg5 protein expression in the cells was detected by Western blotting using anti-Atg5 antibody. GAPDH was used as the internal control. (D-F) Cell viability was determined by MTT assay at 570 nm wavelength for 72 h. Error bars represent mean ± SD. Data were analyzed by Student's t-test. ns: no significant, **: P<0.01; ***: P<0.001.

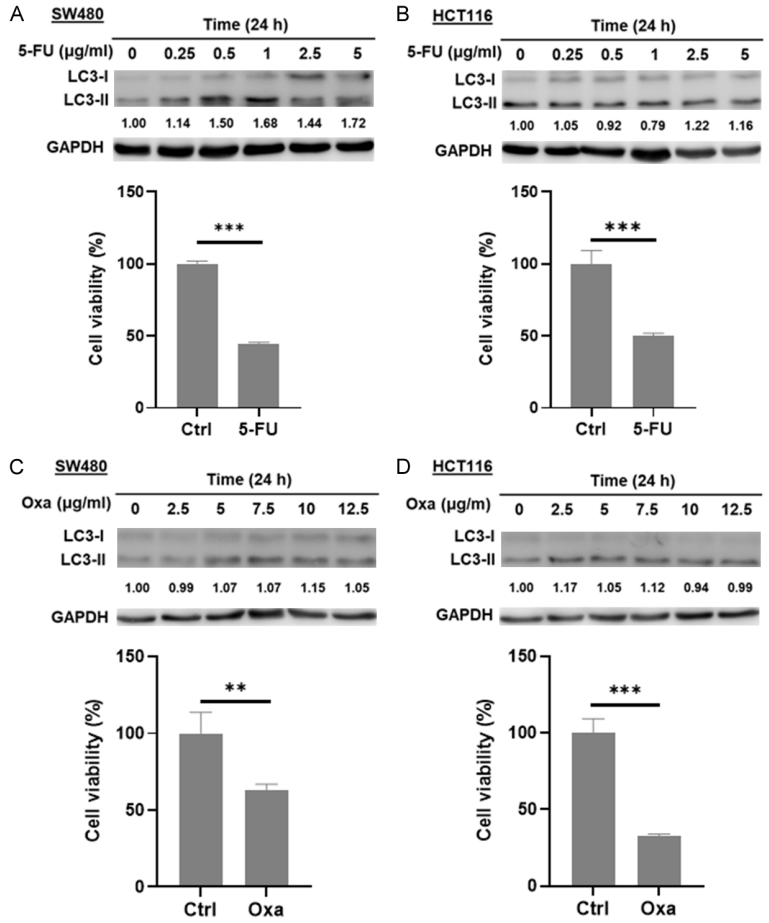

Figure S2. The effect of anti-cancer drugs on the autophagy activity and viability of CRC cells under high glucose conditions. (A, C) SW480 cells and (B, D) HCT116 cells were maintained in different concentrations of 5-fluorouracil

(5-FU) or oxaliplatin (Oxa) for 24 h. LC3 protein expression was evaluated by Western blotting using the anti-LC3 antibody. GAPDH was used as the internal control. Cells were maintained in 1 μg/ml 5-FU or 7.5 μg/ml Oxa. CRC cell lines were treated with anti-cancer drugs for 24 h. Cell proliferation was determined by MTT assay. Error bars represent mean ± SD. Data were analyzed by Student's t-test. **: $P<0.01$; ***: $P<0.001$.

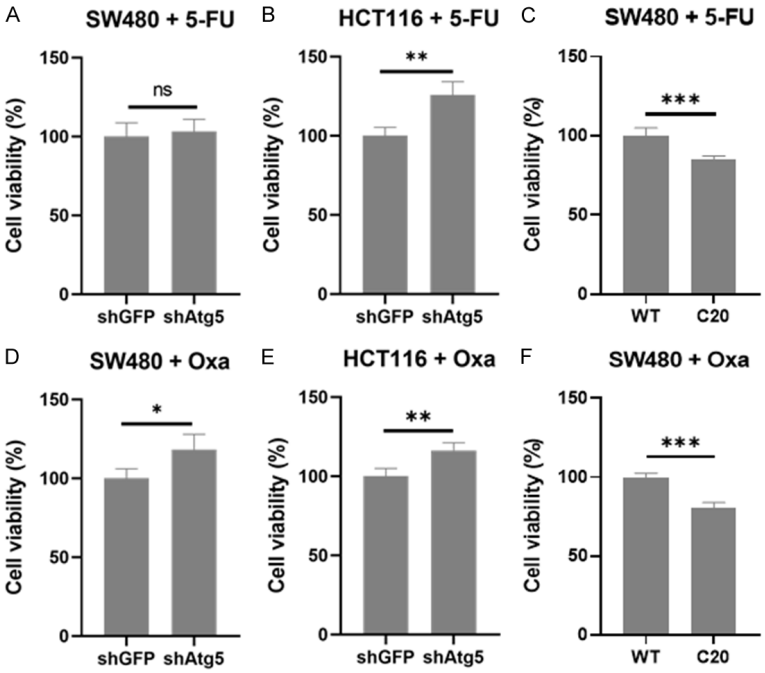

Figure S3. The effect of silencing or knockout *Atg5* gene on the sensitivity of CRC cells to anti-cancer drugs (5-fluorouracil or oxaliplatin) under high glucose conditions. (A, D) SW480 cells and (B, E) HCT116 cells, the *Atg5* gene was silenced by specific lentiviral shRNAs. (C, F) SW480-C20 cells were the homologous recombination by CRISPR-Cas9 knockout *Atg5* gene. Cells were treated with (A-C) 5-fluorouracil (5-FU) or (D-F) oxaliplatin (Oxa). Cell viability was determined by MTT assay at 570 nm absorbance for 48 h. Error bars represent mean ± SD. Data were analyzed by Student's t-test. ns: no significant; *: $P<0.05$; **: $P<0.01$; ***: $P<0.001$.

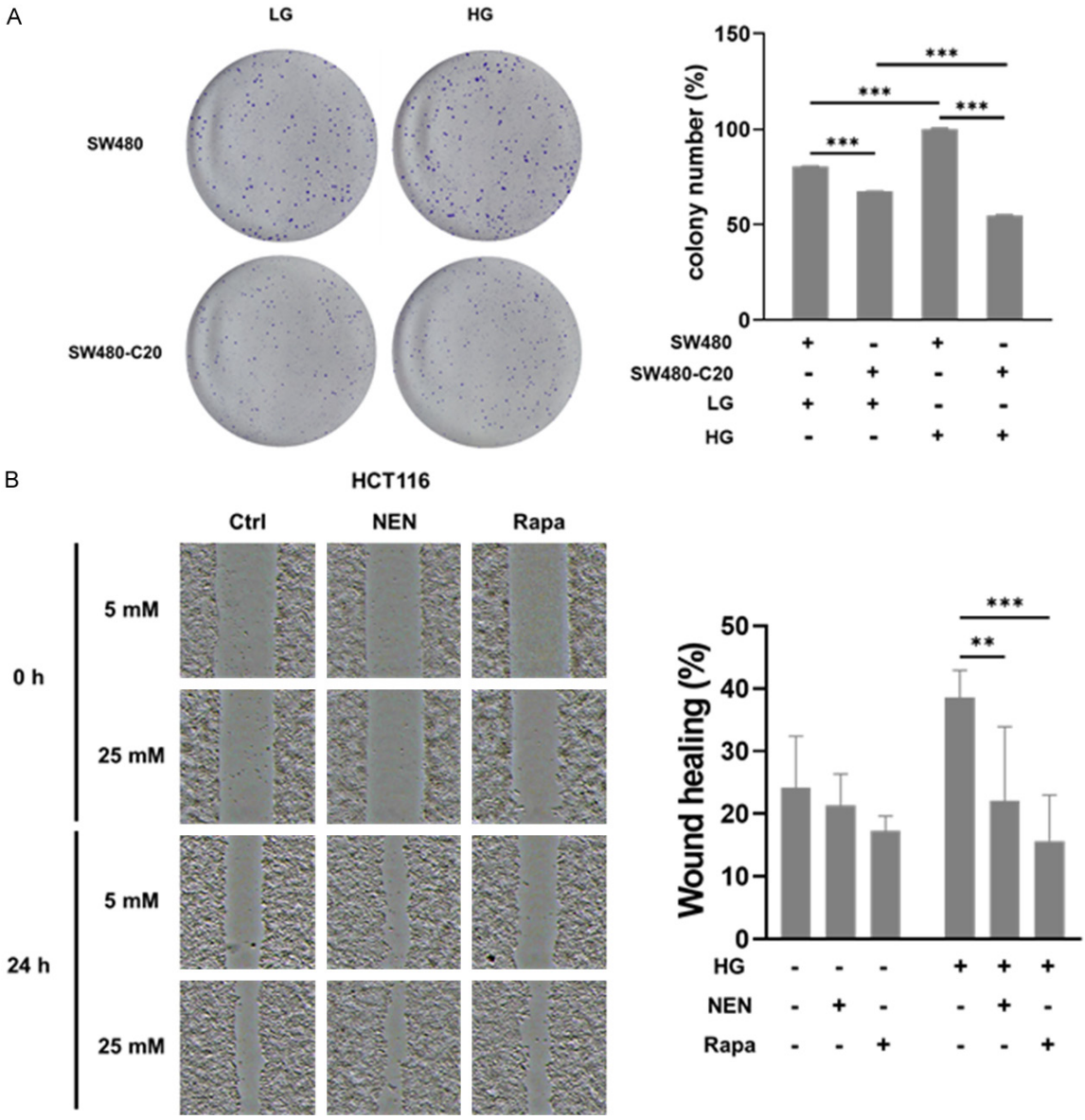

Figure S4. CRC cell focus formation and migration. A. SW480-C20 cell focus formation under 5 (LG) and 25 (HG) mM glucose medium was evaluated at 7 days by focus formation assay. In SW480 cells, the *Atg5* gene was deleted using the CRISPR-Cas9 knockout system to abolish autophagy activity. B. The effect of autophagy on migration of HCT116 cells in 5 or 25 mM glucose medium. The wound healing assay was used to clarify the effect of autophagy on the mobility of HCT116 cells under 5 or 25 mM glucose medium. HCT116 cells were treated with 1 μM NEN or 150 nM rapamycin for 24 h. Then, they evaluated CRC cell migration under 5 or 25 mM glucose conditions at 0 h and 24 h after the treatment of autophagy inducers. Representative images of each group at the indicated time points after gap formation are shown. Quantification is shown in the diagram. Error bars represent mean ± SD. Data were analyzed by one-way ANOVA and two-way ANOVA. **P*<0.05.

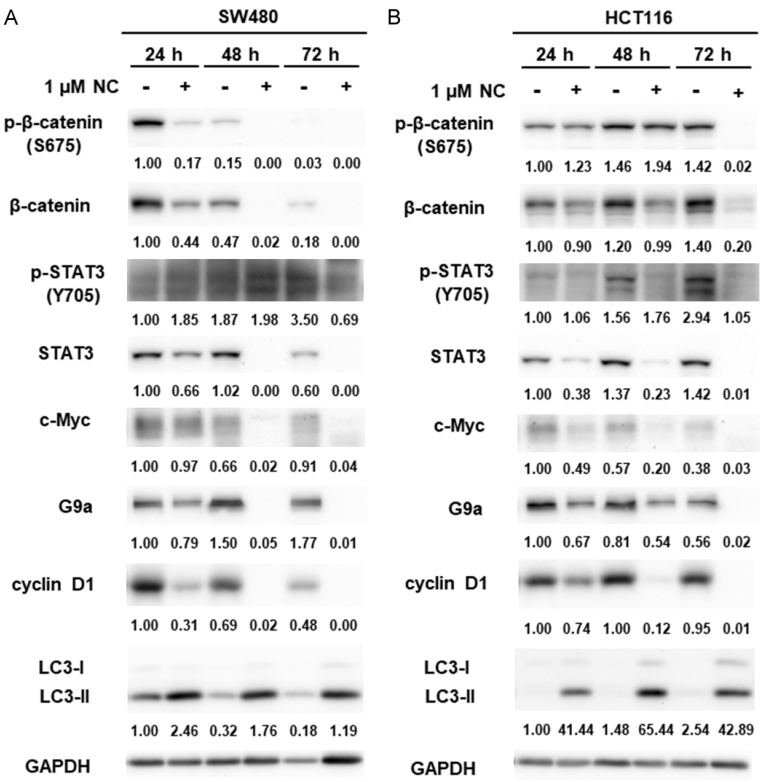

Figure S5. Time course effect of niclosamide on signal pathways of CRC cells under high glucose conditions. (A) SW480 cells and (B) HCT116 cells maintained in high glucose medium were treated with niclosamide (NC, 1 μM) for 0, 24, 48, and 72 h. Protein levels of G9a, β-catenin, phospho-β-catenin (Ser675), STAT3, phospho-STAT3 (Tyr705), c-Myc, cyclin D1, and LC3 were evaluated by Western blotting using specific antibodies. GAPDH was used as the internal control.

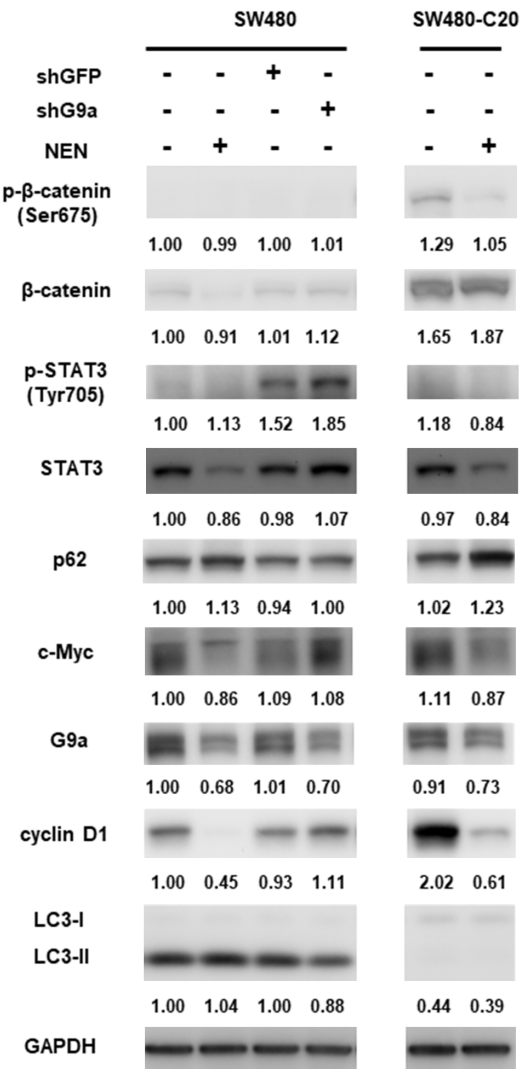

Figure S6. Clarifying the role of autophagy and G9a in related signaling pathways under high glucose conditions by modulating autophagy activity and G9a levels. For suppression of autophagy activity, SW480 cells were cloned by CRISPR-Cas9 knockout *Atg5* gene (SW480-C20). Using genetic silencing of the G9a gene, SW480 cells were treated with lentiviral shRNA to silence the G9a gene. SW480 and SW480-C20 cells maintained in high glucose medium were treated with NEN (1 μM) for 24 h. Protein levels of G9a, β-catenin, phospho-β-catenin (Ser675), STAT3, phospho-STAT3 (Tyr705), c-Myc, cyclin D1, and LC3 were evaluated by Western blotting using specific antibodies. GAPDH was used as the internal control.

Table S1. Characteristics of CRC patients

Parameters	Number
Gender	
Male	124
Female	85
Age (year)	
Range	32-90
Mean	65
<66	104
≥66	105
TNM stage	
Stage 1-2	117
Stage 3-4	92
Recurrence	
Non-recurrence	41
Recurrence	20

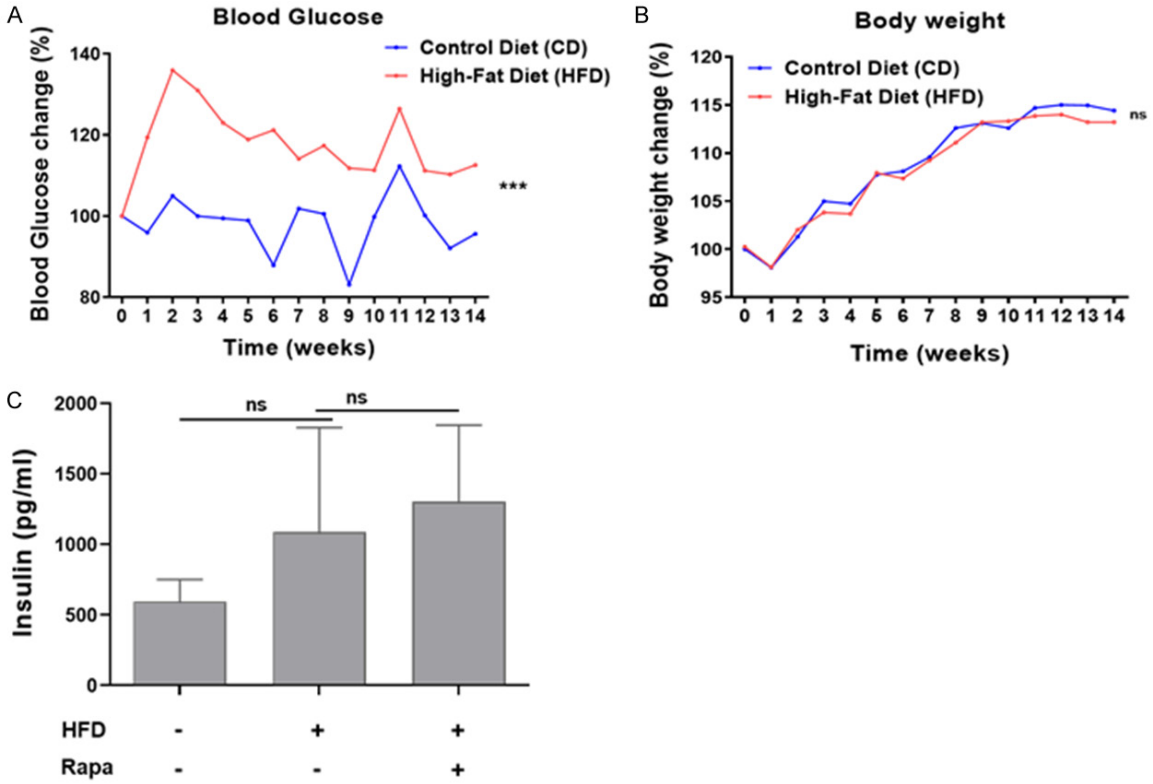

Figure S7. The effect of high-fat diet and autophagy on glucose and the level of blood insulin in xenograft mice. Nude mice were fed a high-fat diet (HFD) beginning at 7 weeks of age. The mice were investigated every week. A. Blood glucose was measured weekly. Statistical significance between groups was determined by the Student's t-test. B. The body weight of the mice was recorded weekly. SW480 cells (2×10^6) were inoculated subcutaneously into nude mice fed with HFD for 11 weeks. Three days after cancer cell inoculation, rapamycin (Rapa, 3 mg/kg) was intraperitoneally injected into the mice every 3 days for 21 days and sacrificed. C. Blood insulin was measured by the ELISA kit. The values shown are expressed as the mean ± SD. Data were analyzed by one-way ANOVA. ns: no significant; ***P<0.001.